ARKIV FÖR FYSIK Band 11 nr 1

Communicated 14 March 1956 by Manne Siegbahn and Ivar Waller

On the isotopic constitution of potassium

A study of mass discrimination in a hot anode ion source

By Carl Reuterswärd

With 12 figures in the text

Contents

I. Introduction 2

1. Problems in determination of absolute isotopic abundance ratio, 2. *2.* The isotope ratios in potassium, 3. *3.* The method of calibration by synthetic samples, 4. *4.* Surface-ionization ion sources, 5. *5.* The scope of the present work, 7.

II. The apparatus 8

1. Geometry of the magnetic analyser, 8. *2.* Mechanical construction of the mass spectrometer, 9. *3.* Electrical equipment, 12. *4.* Vacuum pumps and gauges, 14. *5.* The ion accelerating voltage supply, 15. *6.* The ion-source filament current supply, 18. *7.* The mass-sweep and chart-drive operating unit, 22. *8.* Calibration of the isotope-current measuring equipment, 24.

III. Instrumental errors 25

1. Introductory remarks, 25. *2.* Erratic mass discrimination of ion source, 26. *3.* Influence of beam direction, 28. *4.* Collector efficiency, 30. *5.* Defocusing effects, 31. *6.* Survey of corrections and limits of error, 32.

IV. Measurement of the initial ratio, $^{39}K/^{41}K$ 33

1. Powdered leucite on filament, 33. *2.* Phosphate solutions on filament, 34. *3.* Solutions of natural samples, 35. *4.* Experiments with the atomic-beam ion source, 37.

V. Measurement of the integral ratio, $^{39}K/^{41}K$ 39

1. Theory of fractionating evaporation, 39. *2.* Atomic beam and indirectly heated anode, 39. *3.* Potassium phosphate on filamentary anode, 41. *4.* Discussion of the results on the integral ratio, 42. *5.* Evaluation of the ratio, $^{39}K/^{41}K$, 45.

VI. Measurement of the ratio, $^{39}K/^{40}K$ 46

1. Introductory remarks, 46. *2.* Procedure of measurement, and results, 47.

Appendix 1. Space-charge corrections to peak-ratio measurement 49
Appendix 2. Correction to integral ratio measured, due to incomplete ionization 51
Summary 52
References 53

I. Introduction

I.1. Problems in determination of absolute isotopic abundance ratio

The object of mass spectrometry, within atomic physics, is to obtain accurate measurements of the relative abundances of the naturally occurring isotopes of elements, whether presented as samples of natural composition, or enriched for diverse purposes of research. In many cases, there exists no better method of getting the desired information. The accuracy attained is, then, a matter of general interest, and the methods of checking the results acquire importance.

The relative abundance of two isotopes is given by a ratio number. The determinations of such numbers can be divided in two classes as to the final information sought: absolute determinations, and relative ones; in the case of the latter, only ratios, or small differences of relative abundances in different samples are required. Absolute ratios are relevant in determining the atomic weights of the elements (which are needed for the evaluation of fundamental constants, e.g. e, h), or in obtaining nuclear data, like half-lives of the natural, radioactive elements, or nuclear cross sections. Relative ratios are sufficient for isotopic tracer work, where chemical, etc., processes are studied by using enriched isotopes.

The relative accuracy of measurement of isotope ratios can generally be determined statistically within each series of measurements (the functioning of the instrument being checked by reference samples), and can be rather high, a figure about 0.1 % being common. Concerning the absolute ratio information, the matter is more complicated. Apart from sampling errors, there are added the instrumental errors, which cannot be sufficiently eliminated by the method of variation of parameters; they have to be stated with a certain amount of guesswork. Accordingly opinions often disagree on the absolute accuracy of ratio measurements (Barnard, p. 176).

The systematic errors in question can be classed as follows: (1) ion optical mass discrimination due to faulty design or technique of operation of the instrument; (2) errors of construction or adjustment; (3) errors due to unsufficient knowledge and control of properties of materials, such as variable surface conditions, various processes of diffusion and gaseous transport of the sample substance. With present-day techniques of ion optics, it should be possible to avoid errors of the first class in the case of ions generated at thermal energy; but ions obtained through dissociation of molecular bonds are subject to serious discrimination in ion sources of conventional geometry (Berry). Errors of the second type enter particularly in sources of complex structure, such as the conventional gas ion source (Nier 1947), where close tolerances have to be imposed on slit widths and alignment. The extent of errors of the third type, finally, is difficult to estimate. Evidently design and conditions of operation should be chosen so as to minimize the theoretical uncertainties. The design of the sample leak in a gas ion source requires careful consideration in order to obtain pure molecular or viscous flow. The fractionation of a thermionic-emission (hot anode) ion source has to be investigated individually.

In these circumstances, methods of checking the spectrometer measurements would be welcome. The chemical atomic-weight determination might be one. In the case of two isotopes of nearly equal abundance, take e.g. ^{107}Ag, ^{109}Ag, the expectations are not too bad. 1 % change in the abundance ratio shifts the mean atomic weight by 0.02 %. In the case of a high ratio, however, not much help can be expected from the use of chemical methods. In potassium, 1 % change of the ratio of the isotopes, ^{39}K and ^{41}K, which is about 14, will shift the mean weight by only 0.0035 %. The recent achievements in large-scale isotope separation offer now, for quite general application, the method of calibration by artificial blends, a notable example being given by the work of Nier (1950), which is to be considered in particular in Sect. I. 3.

I.2. The isotope ratios in potassium

The stated points of view can be illustrated by a record of measurements made on potassium. This element has been investigated many times. The interest has had several causes. The element is easily ionized. It has two conspicuous peaks of large relative mass separation (5 %), which makes mass discrimination in ion production and analysis an important factor. It is fairly common in Nature (2 % of the earths crust, 1 % of the salt of ocean water), and it displays a natural radiactivity, which was shown to emanate from the isotope ^{40}K (Smythe & Hemmendinger), of very small abundance.

The results of measurements of the ratio ^{39}K/^{41}K are displayed in Fig. 1. It will be noticed that the statistical errors quoted decrease with time, whereas the discrepancies between different methods become greater. The determination by molecular moment analysis is clearly inferior to the mass spectrometer measurements. Of these latter, the most extensive investigations were made by Brewer. His results, as given for 1936 (Brewer 1936 b, c), display the range of variation of isotopic composition

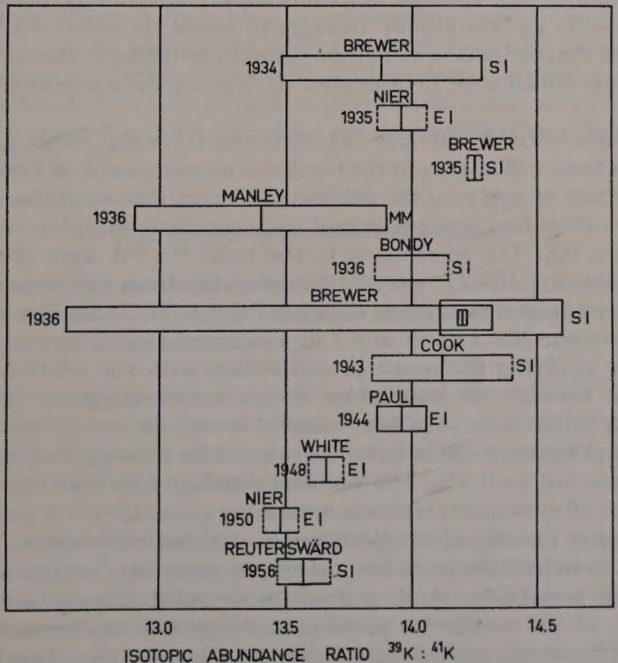

Fig. 1. History of the abundance ratio ^{39}K/^{41}K. The rectangles indicate limits of deviations stated by the authors; continuous lines, maximum limits; dashed lines, probable or average errors.

found in samples of diverse origin: the left frame represents vegetable matter, some sea weeds (Pacific kelps) exhibiting particularly high contents of ^{41}K; the right frame applies to minerals; and the small center frame indicates the results on ocean water, with pertaining limits of error. Common mineral potassium came near the sea water value.

Cook, also working with a surface-ionization ion source, could not corroborate the natural variations found by Brewer; on the contrary, deviations larger than ±0.7 % from a reference sample were not obtained, the relative accuracy being 0.2 % (p.e.). The most probable mean of the ratio, however was in accord with Brewer's.

The results obtained by electron-impact ion sources, of diverse designs, exhibit a marked trend with time (3.5 % between Nier's first and latest result), perhaps indicating a successive improvement in design of the instruments. However, Niers determination of 1950 would claim a particular degree of trustworthiness, being the only one made with a calibrated instrument. The weight of this argument will be examined in next section of this chapter.

The determination of the ratio ^{39}K/^{40}K is, of course, influenced by mass discriminations of the source and of the instrument, however to a smaller degree than the other ratio, since the relative mass difference is only half as large. The earlier determinations are dealt with in a previous publication (Reuterswärd 1951 b).

I.3. The method of calibration by synthetic samples

The importance of this method demands that particular consideration be paid to the measurements by Nier (1950). In order to assess the value of the spectrometer calibration to the determination of isotope ratios in potassium, the results concerning the other elements which were investigated by Nier by the same method will now be examined.

Two instruments (*MS I* and *MS II*), differing in design, were used. Naturally, systematic deviations will appear in the results of measurement; it would be expected, then, that the effect of applying the calibration corrections would be to reduce these deviations. The calibration was performed with synthetic samples, containing about 99 % ^{40}A and 1 % ^{36}A. The corrections to the ratio ^{36}A/^{40}A were about +0.8 % for *MS I*, and +0.3 % for *MS II*, varying considerably from one occasion to another, but in each case being measured to about 0.1 % p.e. In Table 1, now, is given the disagreement between *MS II* and *MS I* in measurements on several elements, both before and after applying the result of calibration with the synthetic sample. The benefit obtained through the calibration is not very impressive, the instrumental differences being reduced in only four cases of seven. However, the differences are small anyhow, and the corrections have the same order of magnitude as the statistical errors, which amount to 0.5 %. The obvious conclusion is that the instruments of Nier have only small systematic errors in measuring gases; they will give good absolute measuring accuracy (mostly about 0.5 %) even without calibration. The calibration can be expected to reduce the instrumental errors somewhat, but not eleminate them, because of their variability which is due, among other things, to memory effects.

Looking, now, at the results for potassium, which was measured in *MS II* only, but with two different slit widths, it is obeserved, that the deviation is considerably outside of the probable error of measurement, and it becomes dubious, that the calibration by the *gas* A really has improved the result on the *vapour* K. Such an issue

Table 1. The effects of calibration on instrumental differences in Nier's measurements (1950).

Isotopes	$\frac{\Delta M}{M}$	Difference $(MS\ II) - (MS\ I)$		Mean correction
		uncorrected	corrected according to calibration	
$^{36}A : {}^{40}A$	1 : 9.5	− 0.49 ± 24 − 0.07 ± 19	− 0.90 ± 36 − 0.33 ± 33	+ 0.73
$^{29}N_2 : {}^{28}N_2$	1 : 28.5	+ 1.10 ± 40	+ 1.00 ± 40	− 0.28
$^{34}O_2 : {}^{32}O_2$	1 : 16.5	+ 0.60 ± 44 + 0.40 ± 50	+ 0.10 ± 50 − 0.15 ± 55	− 0.58
$^{45}CO_2 : {}^{44}CO_2$	1 : 44.5	+ 0.35 ± 35 − 0.15 ± 60	+ 0.25 ± 35 − 0.25 ± 60	− 0.21
$^{39}K : {}^{41}K$	1 : 20	− 0.90 ± 30*	− 1.60 ± 50*	− 0.49

Differences and corrections are given in per cent of measured ratio.

* Measurements made in *MS II* only, the instrument differences given being those of (wide slit)–(narrow slit).

is also understandable theoretically, since the gas is introduced into the ion source in a manner quite different from that of producing a metal vapour; similarly, as regards exhaust by traps and pumps, relevant differences may exist. Furthermore, the great differences in chemical character of these elements make effects of contact potential and secondary electron release on the location of the ionizing electron beam plausible. — Systematic errors can, then, not be regarded as eliminated in Nier's determination of $^{39}K/^{41}K$.

I.4. Surface-ionization ion sources

The ion sources, which are denoted by "SI" in Fig. 1, are by no means of identical construction. Of different SI sources, the following types are conceivable as to the constitution of the emitting surface:

(1) compact solid or molten salt, or oxide (compound thereof);
(2) very thin, possibly not continuous, layer of such, on substrate (Pt, Ta, W, W–O);
(3) clean (or oxidized) surface of metal, impregnated with sample;
(4) metal (or oxidized such) in vapour of sample.

The metallic substrate is heated by the passage of a current, or by heat transfer, or perhaps electron bombardment; the heating is controlled so as to obtain a steady emission. The ions are withdrawn from the surface by an electric field of sufficient strength to overcome space-charge limitation of current.

Brewer, in 1934, used the type (1) (K-Al-silicates), but in the following investigations, type (3); the reason being the better mass resolution obtained, evidently a consequence of the more uniform surface potential. The platinum carrier was impregnated by heating in contact with the sample (Brewer 1935), preferably a silicate or phosphate. Bondy & Vanicek applied the sample (molten glass) to the back of a perforated platinum ribbon; which of the types, nos. (1) to (3), this source belongs to, is not clear. In the present work all four types were tried, the essential measurements being made on no. (2). Recently the type (4) has become widely used (Inghram & Chupka).

In this connection, it will be interesting to calculate the maximum quantity of sample in a monomolecular surface layer on a platinum substrate. This metal exhibits a face-centered cubic lattice with period 3.92 Å. Hence, one cm² contains 1.3×10^{15} atoms. If the adsorbate contains one atom for each of the surface atoms of the substrate, and if the adsorbed atoms are all given off as monovalent ions, then the total charge emitted is 2×10^{-4} As/cm²; from an area, 4 mm², 8 μAs. A good measurement of ^{39}K/^{41}K requiring 10^{-9} A emission, the monomolecular layer will become exhausted in less than 2 hours.

The saturated emission of ions has the following relation to the rate of evaporation of atoms (Copley & Phipps):

$$\frac{i_+}{i_0} = \frac{g_+}{g_0}\,\frac{1-r_+}{1-r_0}\,\exp\left(-\frac{e(I-\phi)}{kT}\right) = \frac{1}{2}\exp\left(-\frac{e(I-\phi)}{kT}\right), \tag{I.1}$$

I being the potential of ionization, and ϕ the electron work function in the layer. It will be assumed that this equation holds identically for isotopes, which is plausible for atomic ions. The isotopic composition of the ion current is then the same as that of the flow of evaporated atoms. The rate of evaporation will be proportional to the concentration of atoms in the layer, and to the thermal velocity as well. Thus, the isotope ratio in the ion current ($q_{12} = [M_1] : [M_2]$) is proportional to the ratio in the adsorbate (Q_{12}):

$$q_{12} = Q_{12}\sqrt{M_2/M_1}\,. \tag{I.2}$$

Hence, the surface-ionization ion source of type (2) exhibits intrinsically a mass discrimination in emission of ions, which is equal to that expected in moleular effusion of a gas through an orifice into vacuum.

In the case of types (1) to (3), the emitted ions, or evaporated molecules, are replaced through diffusion from the interior of the source, or by transport in the surrounding vapour. If the quantity of sample contained in the surface layer is but a small fraction of the total, the isotope ratio of the emitted ions will eventually be determined by their ratio in the bulk sample and their relative speeds of supplying, the fractionation intrinsic with the evaporation becoming immaterial. Thus one could expect the first measurements on a new surface preparation to yield an isotope ratio different from one measured later, when the diffusion has become quasi-stationary. This later one will depend on the ratio of the mobilities of isotopes; in the case of diffusion through a surface coating, mass discrimination may or may not occur, depending on the positions of the diffusing atoms in the lattice (Brewer 1936a). E.g., Li atoms, being much smaller than the interatomic distances in Pt, diffuse interstitially and with fractionation. K and Rb, atoms, however, are large, and they diffuse without such. This conclusion is based on observation of the changes of abundance ratio as the source is consumed; Li giving a variation nearly in accord with the theoretical fractionation ratio, $\sqrt{M_2/M_1}$, K and Rb giving factors nearly equal to 1. Accordingly, the ratios measured for K and Rb on a source of type (3) should be regarded as correct. There remains then, in the case of K, the necessity of explaining the discrepancies with the electron impact source, which are equivalent to a factor M_2/M_1.

The method of preparing sources of type (3) depends on diffusion from a sample substance in contact with the metal surface, at a temperature similar to that used for obtaining the emission; this diffusion into the metal will influence the source fractionation. It is easily understood that in this case a mass-dependent coefficient of diffusion will cause a smaller variation of the isotope ratio during reemission; if the impregnation is superficial only, the variation is nil, but the mass discrimination exists, nevertheless. Also the transport of matter from the sample material, and processes of diffusion within the same, are able to influence the source characteristics. Thus the interpretation of the results obtained by Brewer is uncertain; it is a fact, however, that—in the case of K—there is no great difference in the isotope ratio found in the initial emission of sources of types (1) and (2). This is also evident from a comparison of the results obtained by Brewer, Bondy, and Cook.

The disparity in the results of Brewer and Cook, concerning the natural variations in the isotope ratio, also needs explanation. The large variations of systematic errors in the latter work were assigned to bad vacuum conditions, the accuracy of relative ratio determination being unimpaired through the use of a method of rapid interchange of source filaments. In view of these results, one would suggest that the findings of Brewer might be caused by variations in fractionation due to differences in the crystallographic constitution of the samples.

It will be convenient to distinguish verbally the abundance ratio obtained on a newly prepared source, the *initial* ratio, from the one found by observing the variations during an experiment in which the whole sample is consumed, which we shall term the *integral* ratio. The former differs from the true ratio by the isotope fractionation in the evaporation; the latter can, on certain assumptions, be regarded as free from corrupting effects. The generally accepted isotopic abundances in Li are, in fact, based on an integral ratio determined on a thermionic-emission source of type (1) (Lu). This matter will be dealt with more thoroughly in a later chapter.

I.5. The scope of the present work

Work on potassium started with a set of relative abundance ratio determinations in an experiment of isotope enrichment through electromigration. There being a geological interest in the isotopic abundance of ^{40}K (Gráf), the mass spectrometer was then improved in order to afford better mass resolution and a higher accuracy of isotope current measurement. The results of this work appeared in a short previous report (R I, 1951).

The disagreement of the ratio determinations on potassium, disclosed by the work of Nier (1950), incited then to a study of the fractionation in the surface-ionization source. The method was to repeat the previous measurements of Brewer, with variation of the technique of preparing the ion sources in order to find out possible sources of error and a method of obtaining consistent results of measurement. Constructions of the most simple geometry were chosen in order to avoid effects of variable electric focusing fields. The use of a 180° magnetic analyser, of course, complicated the ion optics in the accelerating space; on the other hand, it reduced effects of the magnetic stray field, which—as a consequence of variations in magnetic saturation of the pole-pieces—affect the isotopic beams differently, since the scanning has to be carried out by varying the magnetic field at fixed accelerating voltage (measurements of such effects are reported by Ehrenberg).

In a realization of a thermionic ion source of type (4) (Sect. I. 4), an atomic beam of potassium was directed onto a clean, heated Pt filament. The effects of filament heating on the geometry of the ion source were then eliminated by constructing an indirectly heated anode. In other experiments, emitters of types (1) and (2) were employed; the type (3) was avoided because of the complicating effects of impregnation. The fractionation of the ion source was determined directly by the method employed by Brewer, viz. by measuring the integral ratio of a sample evaporated to complete exhaustion; such experiments were carried out with the atomic beam source, as well as with salt coatings of different thicknesses. The theory of this method was extended in order to account for a variable degree of ionization as a result of anode temperature variation during the evaporation. However, the mechanism of the thermionic emission of ions from non-metals[1] is not sufficiently well known to make possible an unique interpretation of the data obtained. The intention of settling, finally, the question of the isotopic abundances in potassium through calibration with synthetic standard samples had to be abandoned, since the experimental work was discontinued, owing to external circumstances.

Some results were given in a previous report (Reutersward 1955), and a description of the ion-current measuring equipment appears separately (R II, 1956).

II. The apparatus

II.1. Geometry of the magnetic analyser

For simplicity of construction, the analyser was designed with a 180° focusing field. A magnet of 20 mm gap width, intended for a 5″, 90° spectrometer tube, was available. The poles were remachined to suit a 80 mm, 180° analyser. In order to compensate for the higher field density necessary, the gap width had to be reduced to 12 mm. As this affords rather narrow space for the ion source and collector assemblies, the slits were placed outside the gap, which involves a reduction of the focusing angle. The new field geometry can be regarded as derived from the true 180° case by a small parallel displacement of the field boundary; this merely moves the points of focus transversally to the ion beam (according to eq. (45′) of Herzog; cf. Ploch & Walcher 1950, and Reutersward 1951a). In the present design (Fig. 2), $\Phi = 176°$.

The ions are accelerated in the rather strong stray field of the magnet, and acquire a predeflection before entering the first spectrometer slit; this compensates for the deviation from 180° of the focusing deflection. In practice, the axis of the ion source comes about vertical to the field boundary; means of adjusting the position of the ion source are necessary, however, for eliminating asymmetries of the ion source structure.

The geometry of all the sources used was aimed to give a simple uniform accelerating field. In the case of a ribbon filament (0.1 mm thick, 1 mm wide), this was placed in a somewhat wider slit of a plane focusing electrode, having the center-of-filament potential. Experience indicated the optimum position of the emitting surface to be $\frac{1}{4}$

---

[1] The literature on this subject is rather meagre. Notes on ion emission are found in treatises on electron emission (Reimann, Jones, Wagner). The general physical background of the ion transport in such coatings is dealt with in work on solid state (Seitz) and oxide cathodes (Eisenstein).

slit width within the front plane; sometimes the major part of the emission current thus was made to pass through the first spectrometer slit, 0.27 mm wide. Focusing voltage was tried, but was not used because of its being delicate to adjust and because of magnifying effects of asymmetry in filament position—thus being liable to introduce irregular mass discrimination. In the case of a flat circular disc functioning as emitter, this was inserted flush within a surrounding plane electrode of same potential; no focusing was ever tried with this arrangement.

When measuring the abundance of ^{40}K, it became necessary to improve the resolution by limiting the aperture of the ion beam. Also, in order to prevent grazing reflection of ions at the walls, the beam had to be limited by stops (Fig. 2, *10–11*). In the median plane, the maximum half-angle accepted from the first slit was 0.04 radians. In the direction parallel to the slits, the final limiting is given by the rectangular stop, *11*, the half-angle being 0.006 radians. These stops were then retained for all subsequent work. The second spectrometer slit, *9*, in general was of 0.7 mm width, which results in flat-topped peaks, the mass resolution being limited to 80. In work on ^{40}K, occasionally a 0.3 mm slit was used. The stops and the second slit were aligned to an arc of circle. The exact optimum location of the entrance slit is found by experience; the slit is made easily exhangeable for cleaning.

II.2. Mechanical construction of the mass spectrometer

The magnetic analyser

The spectrometer body (Fig. 2) is constructed of two 4 mm soft iron plates *1*, separated by 12 mm wide brass strips *2*, *3*, which carry flanges and fastenings. These parts are fixed together by bolts, and the chamber made vacuum tight by baked glyptal lacquer, in the way shown by insert I. The entrance slit *8* of the spectrometer is insulated electrically from the housing by mica foils; *9* indicates the mass selector slit, *10* five circular stops, and *11* a rectangular stop (height 6, width 5 mm), which limit the angular aperture of the beam; *12* indicates an insulated slit, which is charged to a negative potential in order to prevent secondary electrons, liberated at *9*, from reaching the ion collector, *13*. All these parts are gold-plated[1] on those surfaces which are exposed to the vacuum. The adopted method of sealing the electrical connections of *8* and *12* into the narrow spaces of the vacuum flanges, is illustrated by insert II. The total leak and gas release in operation was 0.3 l/s at 1 μTorr, as measured by the ionization vacuum gauge. The spectrometer body is suspended in the gap of the electromagnet, and the pole pieces firmly pressed against its sides by means of screw-vices.

The ion source, and the vacuum lock

The ion source as depicted, is mounted for quick exchange in a vacuum lock, which is carried on a mechanical beam directing device, to be described below. The platinum ribbon filament *14* is kept stretched by molybdenum springs, and is mounted abt. 0.5 mm above the plane of the focusing electrode *15*, in the center of the 2 mm wide slit. The filament supporting electrodes and a spring wire, making contact to the adjustable focusing electrode, are fixed in a baked pyrophyllite plug *16*, which is glued to the ion source body *17* by Araldite B (CIBA), this compound also filling the

---

[1] Common commerical electroplating, carried out by Markströms Guldsmeds AB, Uppsala.

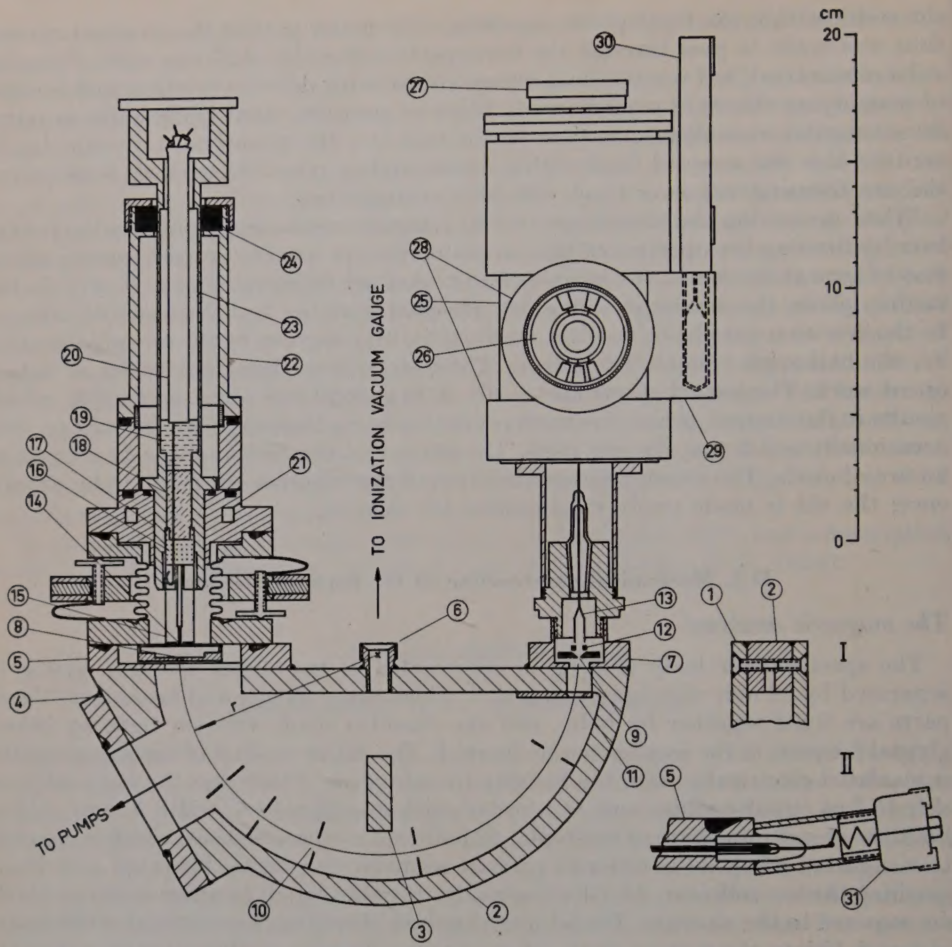

Fig. 2. The magnetic analyser assembly. Scales of inserts are enlarged: no. I, 1.5 ×; no. II, 2 ×.

1. Magnetic pole plates
2–3. Brass separators
4–7. Flanges and vacuum connectors
8. Entrance slit
9. Mass selector slit
10–11. Stops
12. Secondary electrons suppressor
13. Ion collector
14. Filamentary hot anode
15. Focusing electrode
16. Pyrophyllite plug
17. Ion source body
18. Araldite glue type B
19. Soft piceine filling
20. 3-lead cable
21. Water channel
22. Cylinder carrying the ion source
23. Polished metal tube
24. Axial sliding seal (Gaco MIM1835)
25. Preamplifier shielding box
26. Amplifying tube
27. Resistor switching knob
28. Heater elements
29. Copper block
30. Thermometer protecting box
31. Shorting microphone cable connector

bore *18*, thus insulating the outward leads. This inulation is supplemented by a layer of soft piceine[1] *19*, embedding the connections to the cable *20*.

The ion source body *17* acts as the disc of a vacuum valve, making an airtight seal against an O-ring packing in the body of the vacuum lock, which is water-cooled *21*. In order to change the used ion source for a new one, the source is lifted into the cylinder *22*, the polished metal tube *23* sliding in the greased rubber seal *24*. The valve is shut again by means of a valve disc (which is not visible in the sectional drawing of the figure), air is let into the upper compartment of the lock, the cylinder *22* with the ion source assembly removed, and another one substituted. The exact orientation of the filament is thereby determined by a locating stud in the lock housing, engaging in a groove in *17*. Because of the clean, grease-free way of introducing the source into the spectrometer vacuum, the operation is speeded up considerably. With only one operator cleaning and preparing the filaments, and servicing the spectrometer, samples were analysed at a rate of one per hour.

The preamplifier box

This is a brass can *25*, fixed to the spectrometer body, but separated from it by a piece of brass tubing. The amplifier tube is placed in a side tube *26* made of iron for the sake of magnetic shielding. The resistor switch occupies the upper half of the can. For thermostating purpose, the can is covered with electric heating elements *28* and carries a copper block *29*, in which is seated the bulb of a contact thermometer, which is enclosed by a protecting metal box *30*.

The ion beam directing device

The ion beam has to be directed so as to be parallel to the median plane of the magnetic field, passing centrally through the slit *8*, in the direction corresponding to the optimum focusing. The three adjustments are achieved by means of the device which is depicted separately in Fig. 3A, as seen from the left-hand side of Fig. 2. Three axes are visible; there are also three adjusting screws and three balancing springs. Thus, the angle of the beam to the median plane is controlled by rotation about *7*; the direction of the beam within the plane is controlled by rotation about *6*; and rotation about *5* makes the filament move across the entrance slit. The latter adjustments are not exactly independent of each other, because the translation of the filament is accompanied by some beam swinging; and the rotation about *6* will move the beam across the slit, since this is situated below the axis of rotation (cf. Fig. 2). This fact, however, does not much impede the directing of the beam.

The indirectly heated anode

Sources of various designs have been tried. Fig. 3B displays the construction of an indirectly heated anode intended to eliminate distortions of the anode configuration. The aim of the design was to achieve a well-cooled radiation shield *1* in order to avoid heating of the bellows surrounding the ion source. Thus, the anode surface *2* is the only exposed radiating surface. In order to reduce the heat dissipation, the dimensions were kept as small as practicable. The pyrophyllite tube *3* isulating the heater from the anode, was machined to a wall thickness of 0.4 mm. The anode surface was coated electrolytically with Pt on top of a layer of Cu.

---

[1] Ordinary piceine with 10 % lanoline added (von Angerer).

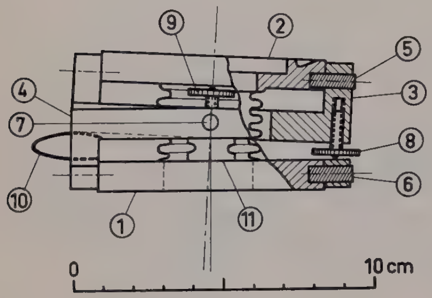

A

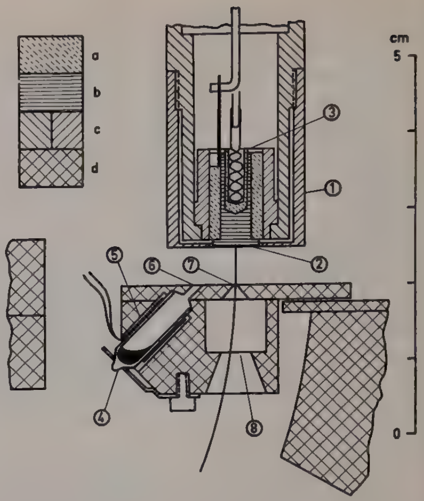

B

Fig. 3A. Device for directing the ion beam.

1. Fixed flange
2. Movable flange, carrying the ion source
3–4. Linking frames
5–7. Pivots
8–9. Adjustment screws
10–11. Balancing springs

Fig. 3B. Indirectly heated anode and atomic beam source. Materials: *a*—baked pyrophyllite; *b*—nickel; *c*—copper, nickelplated; *d*—brass, goldplated.

1. Radiation shield
2. Anode surface, platinized
3. Insulating tube, slotted lengthwise
4. Pyrex crucible
5. Heater winding
6. Atomic beam orifice, 1 mm diam.
7. Entrance slit
8. Ion beam stop

The atomic beam source

The arrangement employed for the experiments with the atomic beam is illustrated in Fig. 3B. The crucible *4*, a small pyrex tube, is fixed radially in the receptacle, so as to avoid making thermal contact with the wall through the heater winding (bifilarly wound enamelled resistance wire).

II.3. Electrical equipment

The magnetic analyser, usually spoken of as *the* mass spectrometer, is, in reality, only the nucleus of a comprehensive and voluminous equipment. A schematic representation of the various components and their interconnections is given in Fig. 4, which is largely self-explanatory. Some points, however, deserve particular mention.

The units *1*, *43*, and *45*, are described in separate sections of this chapter, as is the equipment for producing and measuring the vacuum. The collector current measuring equipment, *25*, *38*, and *39*, is reported on in the paper R II; the data on calibration and evaluation of the readings are dealt with in the following Sect. II.8. The circuitry of the peak ratiometer is, of course, rendered only schematically, omitting, among other things, manual controls. In fact, the switch-timing appliance is here depicted

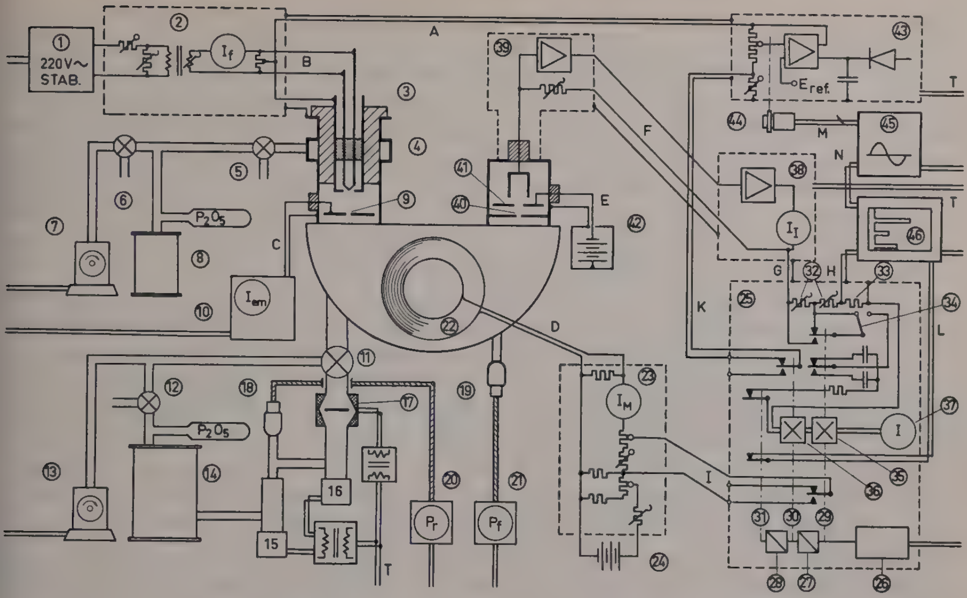

Fig. 4. Diagram of electrical and vacuum connections.

1. Power supply, 220 V ± 0.01 %
2. Ion-source heating-current control circuit
3. Exchangeable ion source
4. Vacuum lock
5–6. Lock vacuum line
7. Rotary oil pumps
8. Ballast tank
9. Entrance slit, insulated
10. Emission monitor
11. High vacuum valve
12. Pre-exhaust line
13. Rotary oil pump
14. Ballast tank
15–16. Oil diffusion pumps
17. Charcoal trap
18. Pirani vacumeter tube
19. Ionization vacumeter tube
20–21. Rough and fine vacuum meters
22. Magnet coils
23. Magnet current control circuit
24. Storage battery
25. Peak ratiometer unit
26. Motor
27–28. Step-up gears, 1:2
29–31. Switch-actuating axes
32. Precision attenuator
33. Load resistor for recorder signal
34. Compare/balance switch
35–36. Current reversing switches
37. Ratiometer balance indicator
38–39. Collector current amplifier
40. Mass selector slit
41. Secondary electrons suppressor
42. "B" battery
43. Ion accelerating voltage supply
44. Mass scanning motor
45. Mass sweep and recorder drive control circuit
46. Recorder

as realized in an alternative way, viz. by an electric motor *26*, driving three sets of switches, *29–31*, through two gears, *27*, *28*, each doubling the speed of rotation (an arrangement employing step-down gears would be preferred in a practical realization). The instrument is set for direct reading and recording of the mass spectrum; by putting the switch *34* in the other position, the circuit is ready for direct peak-height ratio measuring. The interconnections of the units *25*, *38*, and *46*, are slightly different from that given in R II. For clearness, the peak-height comparator unit is left out, and so also are the limit-switch connections of *44* with *45*. The safety system linking the vacuum monitor *20* with the diffusion pumps, the ionization vacumeter and the high-voltage supply, is also left out, as is the arrangement for flushing the preamplifier box with dry air (R II). The ion current intercepted by the jaws of the entrance slit is measured by a direct-coupled amplifier *10*. Its highest sensitivity is 10 $\mu\mu$A to the division; the circuit diagram is substantially that published by Wallenquist for the astrophotometric instrument "Reuterswärd I". All connections labelled "*T*" lead to the output of a "variac" transformer, the voltage being kept constant through manual control.

II.4. Vacuum pumps and gauges

The spectrometer chamber is evacuated through a wide, short channel leading, via a valve *11* and a charcoal trap *17* to the high-vacuum oil-diffusion pump *16*, a *VMF-260* from Distillation Products, Inc., which is boosted by a small $2\frac{1}{2}''$ pump *15* of local laboratory design. Pumping fluids are silicone oil DC703 in the former, and Octoil S in the latter. For good vacuum, the heating power of the high-vacuum pump must be kept constant within $\pm 10\%$; accordingly the heaters are supplied from a tapped transformer, connected to the manually controlled variac. A rough-vacuum ballast tank *14*, a bypass conduite *12* and the rotary oil pump *13* complete the exhaust line.

As discernible in Fig. 4, the charcoal trap is fitted with a central baffle disc, the geometry being such, that any molecule passing the trap has very nearly 100 % chance of hitting the charcoal, which is bounded by a thin net of 0.1 mm wire of Ni. The charcoal is separated from the water-cooled wall by a helical heating wire (1 mm Kanthal). A substantial part of the heating current, however, passes through the charcoal. No refrigeration is used; nevertheless, the charcoal trap facilitates the obtaining of a vacuum better than 1 μTorr. Probably the most important function in this respect is to keep the vacuum fair during the night, when the pumps are shut down; this is equivalent to increasing the ballast tank volume. In the usual routine, the trap is degassed every morning by heating for 10 min and cooling for 1 hour.

A separate vacuum equipment, not appearing in Fig. 4, is employed for the preheating of the filaments; it comprises a *VMF-5* operated with Octoil S, and is equipped with a vacuum-lock. To serve the vacuum-locks, a second rotary oil pump is needed (*7*).

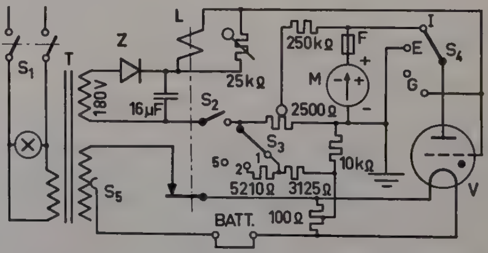

Fig. 5. Ionization vacumeter circuit. *V*—vacumeter tube, Standard 4101D; *M*—meter, 10–0–10 µA; *L*—relay 6019/20VS (Svenska Reläfabriken), adjusted for smaller back-lash (gap reduced by applying a brass foil, 0.15 mm thick); *F*—10 mA fuse; *T*—heater windings: 7–5–3.5–2.5–1.75–1.25–0.9 V, 3 A. The dial of the 2500 Ω potentiometer is graduated directly in terms of pressure, the switch S_3 giving multiplying factors 1, 2, and 5.

The vacuum in the spectrometer is measured by an ionization vacuum gauge mounted directly on the chamber *19*. The electric circuit diagram is reproduced in Fig. 5. The essential features are the following:

(1) The measurement of vacuum is performed by balancing the collector and anode currents; the balance is ascertained by zero reading on the panel mounted meter. Ordinary fluctuations in emission current do not disturb the zero, and measurements can be made with great accuracy and sensitivity to small changes in gas pressure; thus leaks are detected by throttling the exhaust valve, and scanning the vessel walls with a stream of gas (Reutersward 1947). Measuring ranges are extended by reducing the emission current, not increasing the ion current range; thus the damage rendered to the oxide cathode by bad vacuum is reduced. — Direct ion current readings can be obtained by unbalancing the circuit; an external light spot galvanometer can be connected in series with the contact "I" of switch S_4.

(2) The operation of an ionization gauge is made convenient by the automatic control of emission. In the present design this is accomplished in a simple manner by a relay, since the demands on stability are rather small when utilizing the null method.

(3) Leak detection by observing the changes in the emission is possible, if a stabilized mains voltage or storage battery, is available. With the relay operating at a suitable frequency, the changes of cathode emissivity are detected by listening to the periodic clicking of the relay.

On account of a certain liberation of gas in the vacumeter tube, the vacuum gauge is not employed during spectrometer operation. Continuous vacuum monitoring is obtained by a Pirani gauge *18* between the diffusion pumps. For reason of safety, the rotary pumps were not run without supervision. With the ballast tank of 10 l capacity, the diffusion pumps can be run for 6 hours, at least, without rough-vacuum pumping. Lest there should develop a leak, or the cooling water fail, there is installed a safety relay, which is connected to the Pirani gauge through a simple amplifier.

II.5. The ion accelerating voltage supply

The circuit diagram (Fig. 7) was derived from a simple two-tube stabilizer designed according to Hunt & Hickman, originally equipped with a triode-connected, selected 6J7 as the series tube (V_3) and a 90 V miniature dry battery for reference voltage—the screen grid of the amplifier tube (V_4) being fed from a balancing network connecting with the unstabilized high voltage (at point Y of the diagram). Since the power rating (0.75 W) of the 6J7 proved unsufficient in the case of output voltages below 1 kV, and it was realized that pentode-connected tubes would stand a high plate voltage better (Fig. 6a), the circuit was redesigned accordingly. Relevant tube characteristics are reproduced in Fig. 6 b, c. As is easily verified, the ratio of stabilization is

$$S = d e_i / d e_o = x (R_{\mathrm{I}} + \mu_{\mathrm{I}} R_2) S_{\mathrm{II}} \approx x \mu_{\mathrm{I}} R_2 S_{\mathrm{II}},$$

I and II denoting V_3 and V_4, respectively, and x the fraction of e_o applied to the grid of V_4. From Fig. 6 b, c it is seen, that, at $i_{a\mathrm{I}} = 0.3$ mA, and $i_{a\mathrm{II}} = 0.1$ mA, $\mu_{\mathrm{I}} \approx 4000$, and $S_{\mathrm{II}} \approx \frac{1}{3}$ mA/V, making $S \approx x \times 10^6$. Since x is in the range 0.04–0.18, the mains voltage variations through the high voltage rectifier are virtually eliminated. The only problems remaining are those of realizing a sufficiently constant reference voltage, and eliminating the effects of fluctuations in the auxiliary current sources of the supply.

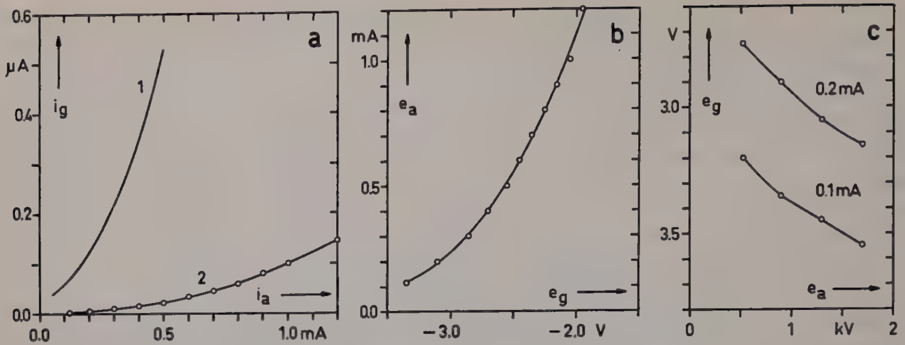

Fig. 6. Characteristics of amplifying tubes.

a. Grid current *v.* anode current. Filament 6.0 V. *Curve 1:* selected 6J7, triode-connected; anode 1400 V. *Curve 2:* selected 6SJ7, pentode-connected; anode 2000 V, screen 42 V.
b. Anode current *v.* grid voltage of 6SJ7. Data as for curve 2 of diagram *a.*
c. Grid voltage *v.* anode voltage of 6SJ7 at different anode currents. Data as above.

Some means of reducing the cathode heating effects of V_4 are necessary for a stability better than 0.1 %. Stabilizing the filament voltage was considered superior to balancing the cathode effects with a cathode-coupled two-tube arrangement (symmetric or non-symmetric, according to Miller), because it avoids the necessity of matching tube characteristics and balance adjustments. Since all filaments are fed from a single transformer, T_2, this was stabilized by a barretter tube, V_1, in series with the 127 V primary. At first, half of the barretter current is passed through a resistor shunting the transformer (at C_1 of Fig. 7). A 10 % slow change in mains voltage would give a 1 % change in the filament voltages. Then, in order to improve the operation, the shunt was disconnected, and 28 % of the transformer core stampings removed. With the whole barretter current now being taken up by the primary winding, the same secondary voltages appear, but as a result of the magnetic flux saturation of the core iron, the slow variations are reduced to 0.3 % for a 10 % mains voltage change. The corresponding effect in the ion accelerating voltage is a change amounting to 0.005 % in the opposite direction. By introducing a shunt capacitance, C_1, the saturation might be carried further, and a still better filament voltage stability obtained.

In order to reduce the sensitivity of the reference voltage to temperature changes, the battery was exchanged for a 85A1 glow discharge tube. This, however, introduced the problem of feeding the 85A1 with a sufficiently stable current. The next delicate elements are, then, the screen voltage of V_4, and the supply of the 85A1. Both having to be stabilized, this function is effected by a voltage regulator tube, V_5, which is fed through a rectifier from the filament current transformer, thus sharing the benefit of primary long-time stabilization. Short-time fluctuations of the mains voltage, however, are not reduced substantially, and it is necessary to improve the performance by providing means of balancing the opposing effects of the screen and cathode voltages of V_4 on the resulting ion accelerating voltage, e_o. This balance is achieved by the network R_5–R_{10}, which needs some adjustment, according to the magnitude of e_o, by R_8, the dial of which may be graduated in e_o.

The difficulties of obtaining constant auxiliary currents for this stabilizer arise from the fact that the highly stabilized output voltage is inapplicable internally,

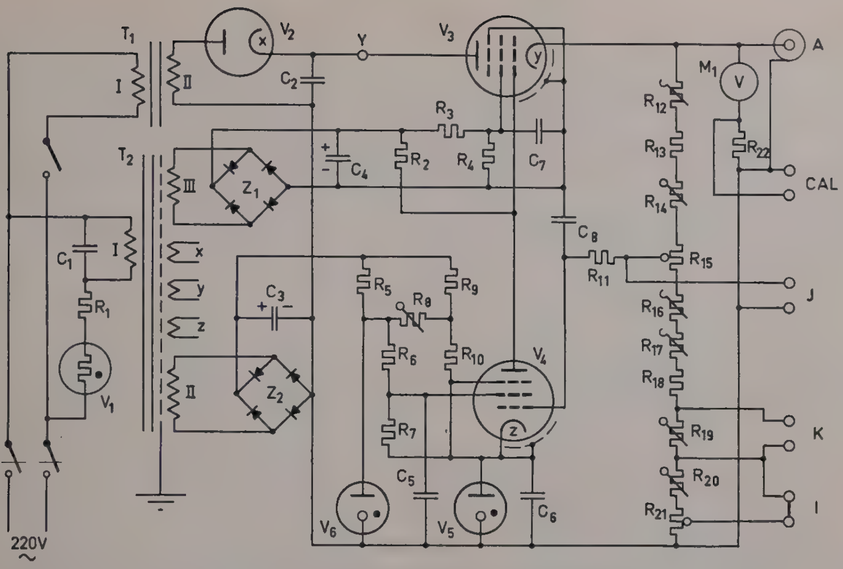

Fig. 7. The ion accelerating voltage supply.

V_1	C10	R_1	100 Ω	R_{12}	12 × 500 kΩ var.
V_2	2X2	R_2	1 MΩ	R_{13}	500 kΩ
V_3–V_4	6SJ7	R_3	68 kΩ	R_{14}	600 kΩ var.
V_5	85A1	R_4	33 kΩ	R_{15}	50 kΩ pot. lin.
V_6	150A1	R_5	68 kΩ	R_{16}	10 × 50 kΩ var.
C_1	see text	R_6	200 kΩ	R_{17}	10 × 5 kΩ var.
C_2	0.5 μF, 3 kV =	R_7	100 kΩ	R_{18}	200 kΩ
C_3	16 μF, 400 V =	R_8	250 kΩ var.	R_{19}	25 kΩ var.
C_4	8 μF, 250 V =	R_9	100 kΩ	R_{20}	10 kΩ var.
C_5	1000 pF	R_{10}	83 kΩ	R_{21}	20 kΩ var.
C_6	0.1 μF	R_{11}	470 kΩ	R_{22}	5 kΩ ± 1 %
C_7	5000 pF	Z_1–Z_2	B250C90 (Siemens)	M_1	0–2 kV =, 10 MΩ
C_8	2000 pF, 2 kV =, ceram.				

T_1 TS-5950 (AB. Svenska Elektromagneter, Åmål);
I: 220 V: *II:* 2500 V.
T_2 No. 114334 (Elektrotekniska Verkstaden, Åkarp), modified;
I: 127 V, 0.2 A; *II:* 230 V; *III:* 115 V; *x:* 2.5 V; *y–z:* 6.3 V.

Panel-mounted connectors:

A	output 500–2000 V, max. 0.75 mA (see text)
CAL	calibrating output, 0.12–1.00 V
J	peak top scanning input
K	base control input for peak height ratiometer
I	electrical peak switching control input (shorted when not in use).

because it is variable in operation; nor are there any simple means of procuring a constant current from it by coupling switches to the elements which control it, these elements being arranged in a manner to easily define the equivalent ion mass, which varies inversely as the output voltage. The knob dials of R_{15}–R_{21} are graduated directly in mass units (one for each 10 kΩ of resistance), and the ion mass is obtained by addition of the dial readings. The mass spectrometer is subsequently tuned by adjusting the ion accelerating voltage by means of R_{12}, R_{14}, these carrying arbitrary dial divisions. A linear mass sweep is then achieved by the motor-actuated potentiometer R_{15}.

If the switched or variable resistors R_{16}–R_{21} were duplicated and connected in a put-and-take potentiometer fashion, the linear range of mass shifting would be extended. However, the possible mass changes are limited by the power-carrying capacity of the series tube (2 W being supposed safe maximum) and of the resistors R_{12}–R_{14}.

First, the units of R_{12} (nominally rated at 1 W) should not be loaded with more than 0.5 W, i.e. 1 mA. This gives:

$$\text{mass number } M \geq 8.5.$$

Second, with 2800 V on C_2, and the output current negligible, the minimum mass number allowed by power dissipation in V_3, at output voltage e_o, is given by:

$$M \geq 8.5 \cdot \left(\frac{2000}{2800 - e_o} - \frac{e_o}{10\,000}\right)^{-1}.$$

For $e_o = 1000$: $M \geq 8.5$; for $e_o = 500$: $M \geq 10.5$.

Third, the limited resistance range of R_{12}–R_{14} sets the following maximum to the mass:

$$M \leq 50000\ (e_o - 85)^{-1} \leq 123, \text{ for } e_o \geq 500 \text{ V}.$$

Outside these limits, the ion mass number has to be applied to the dials with some scaling factor.

The stabilizer has also been used without the rectifier Z_2, the tubes V_5, V_6, and adjoining network being fed from point Y through two dropping resistors, composed of several 5 MΩ, 2 W units connected in parallel. However, in this way, rather large variations were introduced into the balancing circuits and could not be balanced completely, a mains voltage effect amounting to 0.02 % remaining in the output voltage. With a reasonably constant mains voltage, however, the supply operated sufficiently well. In a test for the over-all stability of the mass-spectrometer system, the largest fluctuations in mass scale observed during 10-minute periods were 0.0036 %. However, during runs through some hours, variations of 0.1 % were encountered. The dropping resistors mentioned were liable to give trouble. Different makes tried (Alpha, Vitrohm) would operate satisfactorily for some hundred hours but eventually fail, possibly due to the confined space allowed to them in the chassis. All other resistors of the stabilizer (except R_1) are common deposited carbon resistors and have behaved well, as long-time stability has not been essential. The resistors of the ratio network, R_{12}–R_{21}, are all spread out on the front of the panel, and the chassis is separated therefrom by a slit 4 cm wide, allowing easy free flow of cooling air.

II.6. The ion-source filament current supply

The thermionic emission is extremely sensitive to changes in the heating current (Sect. V. 5). Thus a filament current supply stable to 0.01 % during 10-minute periods is necessary. Experience with storage-batteries proved the controlling rheostats to be a serious problem at these high currents (5 A) and low voltages (2 V),

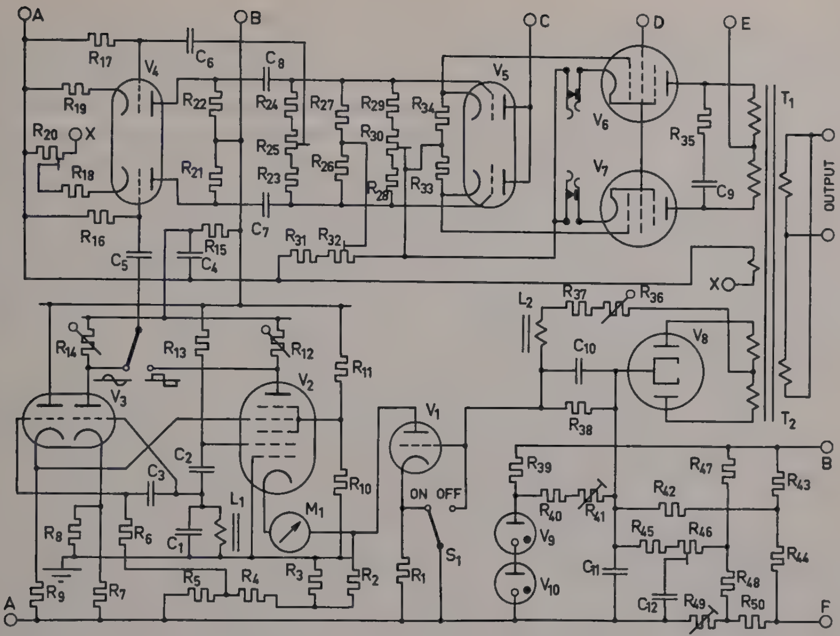

Fig. 8. Stabilized 220 V a.c. power supply.

V_1 6J6
V_2 6A8
V_3 6SN7GT
V_4 6SL7GT
V_5 6SN7GT
V_6–V_7 6L6
V_8 6H6
V_9–V_{10} 85A1
M_1 0–10 mA =
L_1 5 H
L_2 500 H
C_1 0.25 μF
C_2 0.5 μF
C_3 0.1 μF
C_4 8 μF
C_5–C_6 50 000 pF
C_7–C_8 0.1 μF
C_9 500 pF
C_{10} 32 μF
C_{11}–C_{12} 8 μF

R_1 1 kΩ
R_2 10 kΩ
R_3–R_4 50 kΩ
R_5 1 MΩ
R_6 500 kΩ
R_7 150 kΩ
R_8 68 kΩ
R_9 50 kΩ
R_{10} 10 kΩ
R_{11} 15 kΩ
R_{12} 25 kΩ var.
R_{13} 50 kΩ
R_{14} 100 kΩ var.
R_{15} 2 kΩ
R_{16}–R_{17} 500 kΩ
R_{18}–R_{19} 1 kΩ
R_{20} 100 Ω
R_{21}–R_{22} 50 kΩ
R_{23}–R_{24} 500 kΩ
R_{25} 250 kΩ

R_{26}–R_{30} 500 kΩ
R_{31}–R_{34} 50 kΩ
R_{35} 30 kΩ
R_{36}–R_{37} 25 kΩ
R_{38} 100 kΩ
R_{39} 20 kΩ
R_{40}–R_{41} 100 kΩ
R_{42} 5 MΩ
R_{43} 100 kΩ
R_{44} 300 kΩ
R_{45} 2 MΩ
R_{46} 1 MΩ pot.
R_{47}–R_{48} 100 kΩ
R_{49} 500 kΩ var.
R_{50} 100 kΩ
A −100 V stab.
B +150 V stab.
C +150 V stab.
D +250 V stab.
E +335 V
F −210 V

T_1 2 × 195 V, 40 VA/220 V, 25 VA/7.2 V, 6 VA.
T_2 220 V/2 × 250 V, 10 mA.
S_1 Stabilization on/off switch; S_2 Sine-wave/square-wave switch.

because of heating of the sliding contacts and irregularities of the wire surface (the rheostats were made of Kanthal wire of 3 mm diameter). Also, the need of charging and maintenance of the batteries was found annoying. The alternative is an electronically regulated a.c. supply, where controls can be operated in the primary circuit of the step-down output transformer. The most common way of realizing it, is that of inserting a regulating device in series with the a.c. mains voltage. Rapid fluctuations of the latter are, however, passed by the regulator with little attenuation, and an unbalance detector in the stabilizing unit must first sense the fluctuation before causing the regulator to operate. Difficulties arise in separating the unbalance component from the mains frequency signal in a sufficiently short time, and because of the rapidity with which the filament ribbon follows the heating current, a perceptible part of the original fluctuation will occur in the ion current. In order to avoid these difficulties, the mains power was first converted to d.c., stabilized and filtered as desired, and then, by means of a regulated oscillator, reconverted into a constant alternating voltage, from which the filament current is obtained. The filament supply is thus made to function as a source of constant 220 V a.c., and can be employed as such for various laboratory purposes; the maximum power output is 30 W. The circuit diagram appears in Fig. 8.

The principal features are the following. A heptode (V_2) is operated as a transitron oscillator in a circuit with a stabilized supply voltage. A square-wave can be extracted from the plate circuit (or a sine-wave from the tank circuit, L_1C_1, by means of the amplifying stage comprising one section of V_3), and is amplified in a feedback-amplifier with two 6L6:s in a class AB:2 output stage. A small transformer and rectifier circuit, connected to the output, converts the alternating output voltage to a direct voltage, part of which is compared with the fixed 170 V reference voltage derived from two 85A1:s. The difference is amplified in V_1 and regulates the cathode bias of V_2 in such a way as to change the amplitude of oscillation in the correct direction, thus maintaining a very nearly constant output voltage, irrespective of fluctuations in the mains voltage, or variations in amplifier tube characteristics, or load. Some qualifications of this statement are, however, necessary.

The magnitude of the output voltage is assessed through rectifying with a choke-input ripple filter, which results in an *arithmetic* mean, and not the *root-mean-square*, which is directly representative of the heating power in the filament. There thus results the requirement, that the wave shape be unaltered when the oscillator is controlled through the feed-back action. The mode of controlling the V_2, by the cathode potential, with fixed screen and space-charge grid potentials, is chosen for a maximum range with a minimum distortion; to this end, a part of the cathode excursion is transferred to the driving (no. 4) grid via a cathode-follower (left section of V_3).

The object of the a.c. amplifier (V_4–V_7) is to reproduce the oscillation applied to the input grid of V_4 (the amplification of the sine-wave in V_3 is linearized by a certain amount of local feed-back), irrespective of fluctuations in the unstabilized plate current supply of the output stage, or in other accessory current supplies. This is necessary, because rapid disturbances will not be eliminated by the d.c. comparison between V_8 and V_1. The amplifier is, therefore, stabilized by negative feedback from a secondary winding (X) of the output transformer to the input cathode of V_4. However, the amount of feedback employed is restricted by parasitic oscillations, both the amplifier and the output transformer being too primitive to offer "hi-fi"-performance. Thus the effect of mains fluctuations are reduced about 10-fold, but not practically eliminated.

The heaters of V_1 and V_8 are fed from the stabilized output at X, and thus do not introduce any source of error in the d.c. comparison circuit. The supply of V_9–V_{10} does, however, the reference voltage becoming in a small degree dependent on mains voltage. In order to cancel this as well as the other small influences, the reference voltage was corrected by a network (R_{40}–R_{50}, C_{11}–C_{12}), introducing a balancing signal, which is derived from the negative end of an unstabilized 360 V = supply voltage (F). The balance is adjusted independently for fast (R_{41}) and slow (R_{49}) mains voltage changes, and the time-constant of the slow compensation is adjustable, too (R_{46}).

For measuring the "noise" and drift of the output voltage, two methods were used. First, the saturated emission from a metal filament diode (Philips 1875) was measured in a balancing network, and the variations in emission current displayed by a Honeywell-Brown potentiometric recorder. By this means, the ordinary fluctuations are measured, and the adjustments for balancing the mains voltage effects checked. The long-term stability cannot be assessed by this device, since the diode exhibits substantial drift of characteristic. Instead a simple half-wave rectifier, consisting of a 6H6 and a RC ripple filter, was used in connection with a precision potentiometer bridge, measuring the rectified current. This method is, of course, not completely reliable, but means of measuring rms values of a.c. to 0.01 % are not easily procured. Some results of the measurements follow:

(1) With no reference-voltage correcting network, the ratio of stabilization was 1:0.0065 for 50 % of max. output load (26 W), and 1:0.0095 for 83 % load.

(2) The reference tubes, V_9–V_{10}, being supplied from an external constant current source, the ratio of stabilization rises to 1:0.0035 for a 50 % load.

(3) With the correcting network according to Fig. 8, the output voltage, at fixed load, can be made independent, to 0.005 %, of fast or slow mains voltage changes within the range 210–240 V, the ratio of stabilization thus being larger than 1:0.00015. The correcting network, however, cannot reduce the sensitivity of this ratio to load changes, which is given by the result of the measurement (1).

(4) With the load increasing from 50 % to 83 % of max., or from 60 to 100 mA at 220 V, the output voltage falls 0.35 %, which is equivalent to 18 Ω of internal resistance.

Regarding the two feedback loops, the following data were collected:

I. The a.c.-amplifier feedback.—The gain of the output stage being strongly dependent on the load resistance, the maximum feedback voltage to be taken from the resistor R_{20}, is determined by the output current. With a minimum resistive load of 60 mA (i.e., 50 % of max.), the full 7.1 V at X may be employed; the loop gain is then 9.

II. The over-all feedback.—The loop gain was calculated from the following data, applying to sine-wave oscillations: (1) the dynamic transconductance in V_1 is 2.8 mA/V; (2) the cathode input resistance of the oscillating V_2 is 1.2 kΩ; (3) the control factor of sine-wave oscillations is: 26 % of amplitude per volt of cathode potential swing; (4) the d.c. unbalance signal is 1.7 V per percent of output voltage. The loop gain is the product of these four figures, viz. 15.

The power output is limited by the maximum safe dissipations in plates and screen grids of the output tubes, and the circuit is designed to allow ± 10 % variations in the mains voltage without exceeding the maker's ratings. Theoretically, the maximum power output is 39 W (335 V plate and 250 V screen, with 182 mA plate, 14 mA screen, and 4 mA grid current, the plate loading being 1000 Ω at 195 V ~), but actually, not more than 26 W could be extracted, 6 W being consumed in the heating of V_1 and V_8; the remaining 7 W represent transformer losses. The prerequisite for this high exploitation of the output tubes is the maintenance of the proper operating conditions. This purpose is served by the balancing network R_{23}–R_{34}, the measuring jacks in series with the cathodes of V_6–V_7, and means (not shown in Fig. 8) of controlling the heating current of each of these tubes individually. Thus, with the feedback loop intercepted, the a.c. amplifier is trimmed: (1) for symmetrical output stage driving signals (R_{25}); (2) for equal grid bias on both output tubes (R_{30}); (3) for correct zero-signal cathode-current (R_{32}), and symmetry of cathode currents (by adjustment of the heater currents). With the feedback loops closed, the output voltage is set by R_{36}, and the oscillator current adjusted to 3.25 mA by R_{14} (or R_{12}, if square-wave oscillations are employed). The frequency of the oscillator shown is 180 Hz.

II.7. The mass-sweep and chart-drive operating unit

In order to record the whole potassium spectrum properly, the mass scanning had to be carried out with a variable speed, and interrupted and restarted at any instant. In ordinary work—without changing of the amplifier input resistor—the chart movement should be started and stopped simultaneously with the mass sweep, and there is also some need of rapid change of the chart speed. Some kind of mechanical coupling and gearing of the scanning potentiometer and the paper feed mechanism is an obvious, and probably the best, answer to these requirements, but would necessitate reconstruction of the recorders employed. A different method was therefore chosen, avoiding the mechanical linkage between the movements and, in addition, providing the means of starting and stopping without any switching arcs and h.f. disturbances to the amplifiers.

The mass sweep is performed by a 1 rpm geared Bodine motor, this as well as the chart driving motor of the recorders being of self-starting synchronous type, which can be made to run on frequencies below the design frequency, 50 Hz. Fig. 9 A gives the schematic of a unit, in which a thyratron relay is used to "gate" half-period waves from the a.c. mains in such a way as to simulate frequencies of 50/3, 50/5 etc. The functioning will be understood by referring to Fig. 9 B, which displays the waveforms appearing in different points of the circuitry, in the case of a 50/3 Hz output.

The pulse timing stage is a cathode-coupled clipper circuit, driven by 250 V ∼ (*a*) applied to the input grid through the 1 MΩ current-limiting resistor. The 50 Hz square-wave voltages (*b*) obtained at both plates of the first tube, are differentiated to yield 100 μs pips, of which only the positive ones actuate the cathode follower of the pulse shaper (*c*). These pulses trigger pulses in the following stage (*d*), which becomes blocked for intervals determined by the capacitance C. At the begin of every blocking period, a positive pulse is transmitted to the next stage, there generating a gating pulse (*e*) for the thyratron switching circuit, which accordingly passes one half-period of mains current (*f*) to the output transformer.

It is essential that pulses of alternating polarity appear at the output transformer, because, otherwise, the core thereof will receive d.c. magnetization with resulting large magnetization current, which will destroy the thyratrons. Such a case will occur if the timing of the blocking pulses becomes faulty. The circuit of the blocker is, therefore, designed for maximum stability, being supplied by VR-tube stabilized voltage and having the "tank" circuit free from external connections. The return of the grid leak is to the positive supply, which also stabilizes the blocking period against changes in cathode potential. Thus, blocking time, t_B, is exactly proportional to the product RC, in which R is adjusted and then kept fixed, but C exchanged by a switch to give the desired interval $t_B = 0.01\ (2\,n + 1) - 0.008$ s; the 0.008 s interval

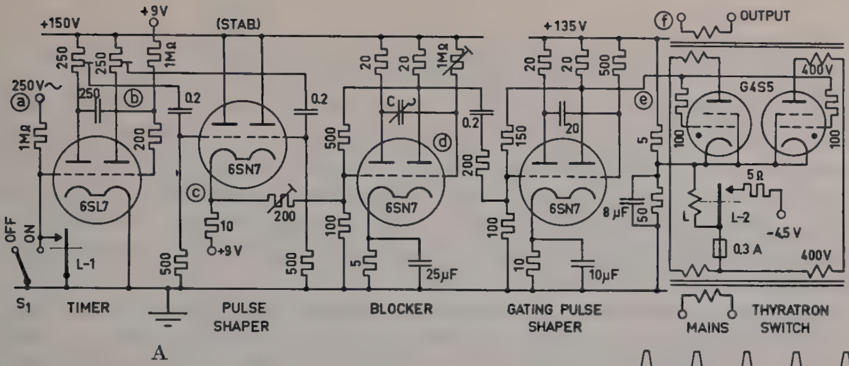

Fig. 9A. Circuit of mains frequency divider. When not otherwise indicated, resistances are given in kΩ and capacitances in mμF. $C = 0.02$–0.1–0.21 μF, for output frequencies 50–50/3–50/7 Hz. L is a 2.8 V d.c. relay shunted to trip at 0.3 A.

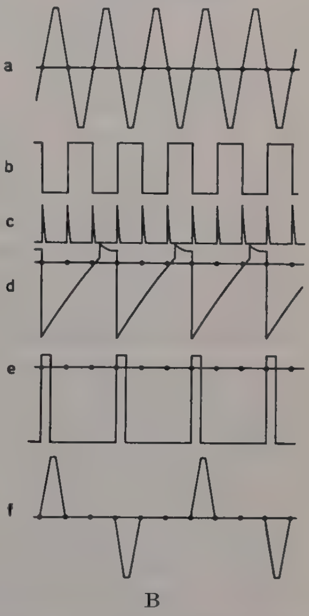

Fig. 9B. Wave forms generated within the frequency divider.

a mains voltage
b voltage on left plate of pulse timer
c cathode voltage of pulse shaper
d voltage at right grid of blocker
with common abscissa axis
e grid-to-cathode voltage of the thyratrons
f output voltage

being left for recharging of C through the cathode circuit. However, if some fault should occur, the thyratrons are protected by the relay L, which in case of overload: (1) with one contact (L-1) interrupts the generation of timing pulses; (2) with another contact (L-2) connects itself to a holding current and thus stays in the actuated position until the mains current is switched off by the operator. Parallel to L-1 there are, besides manually operated contacts for on/off control of the load, limit switches at the scanning potentiometer.

The unit constructed thus, contains two separately controlled thyratron gates, supplying two channels of max. output 65 VA each. The experience is, that operation on 50/3 Hz is proper, but on 50/7 Hz uncertain. Some motors will not run at all at this low frequency; others have to be started on a higher frequency, and will then run on the lower, but at a too high speed, performing an act of frequency multiplication of their own. The range of operation is thus quite limited, but within its limits the unit functions well and has given no troubles, the starting and stopping of the motors giving no disturbances in the ion current records.

II.8. Calibration of the isotope-current measuring equipment

A detailed description of the direct-coupled amplifier used for measuring the separated isotope currents, together with an account of several methods of calibrating the instrument, is published separately (R II). There are also given some results of measurements on the amplifier gain and the linearity of characteristic of the resistors used. They indicate the response of the instrument to be linear to 0.1 % within all ranges employed, thus making corrections unnecessary in all ordinary mass spectrometric work.

When operating with the peak ratio meter, a much higher precision is attainable, theoretically. In this case, the output circuit of the amplifier is subject to a constant load, equal to the input resistance of a 10 kΩ decade potentiometer. The amplifier gain is then so high, and constant, that no correction for illinearity would be necessary in this case, either.

Accordingly, the only information necessary for evaluating the meter reading in terms of input current are the following: (1) linearity error of meter scale; (2) range of meter considered as voltmeter; (3) resistance of input resistor. These factors will now be considered in some detail.

(1) The instrument mounted on the amplifier panel was calibrated several times and the corrections found reproducible within 0.2 % of range. Two recording instruments were employed: an Esterline-Angus recording galvanometer of range 1 mA ("EA"), and a Honeywell-Brown potentiometric recorder, with 2.5 mV range ("HB"). The former was preferred for the work on ^{40}K because of the greater speed of response (1 s); in order to obtain this it was, however, necessary to install a device for reducing the friction between pen and paper (see R II). The scale was not linear, and the deviations were very sensitive to the mounting of the instrument, variations of 0.5 % occurring; therefore, the scale was calibrated (method B1 of R II, sect. II.6) repeatedly in the course of the ion current measurements. The HB recorder, however, has a response linear within 0.1 % and is preferred for ordinary work, where the speed of response, 4.5 s, is sufficient.

(2) The voltage ranges were, in the case of the internal multiplier rheostat, evaluated by the method A2 of the cited reference, the accuracy attained being 0.1 % or better, for all ranges from 0.1 to 10 V. The decade potentiometer of the ratiometer circuit was, of course, calibrated directly, in a precision Wheatstone's bridge.

(3) The input resistors, being calibrated according to the method, B1, cited, showed irregular variations. The measurements on ^{40}K, which involve the comparison of currents measured by different resistors, are not quite as accurate as the others, since calibration of the resistors were not made in direct connection with the current measurements. Here follows a record of the ratios obtained for the two resistors used:

Date:	8/2	13/2	14/2	2/3	11/3	12/3
R_3/R_1	71.03 ± 10	71.31 ± 10	71.25 ± 10	71.79 ± 10	71.56 ± 50	71,74 ± 10

From this is obtained the mean: 71.45 ± 14, the individual probable deviation being ± 0.25, or ± 0.35 %.

III. Instrumental errors

III.1. Introductory remarks

In the investigation of the discrimination in the emission from ion sources, it is essential that the isotope separation and measurement does not introduce any systematic error. In an ideal magnetic analyser, all the emitted ions are brought to the collector in the course of a measurement, and the task of isotope ratio determination reduces to one of beam collecting and electrical precision measurement of small currents. On account of ion optical limitations, however, in practice only a small part of the ions are collected, and various criteria must be sought regarding the absence, or limits, of discrimination.

The main cause of the low efficiency of ion collection is the lack of ion optical focusing of ion tracks, which are oblique to the median plane of the magnetic field. Also, the focusing errors of the median-plane ion optical system demand some limitation of the beam width, in particular as second-order focusing is not obtained in the 180° geometry used. The following calculations are to assess the fraction of the ions which are rejected by the aperture limiting stops.

According to the Boltzmann law of molecular energy distribution, thermal energies (due to translation in one coordinate), which are greater than $e\,U_{th}$, are acquired by the fraction $\exp(-e\,U_{th}/k\,T)$ of the ions emitted at the temperature T. The accelerating field was approximately uniform. If the velocity component considered is at right angles to the beam axis, the resulting ion track obliquity angle is $\theta \approx \sqrt{U_{th}/U}$, where $U \gg U_{th}$ is the accelerating voltage. The virtual point of origin of each pencil of rays is, in the case of a uniform field, in the plane at distance d within the emitting surface, d being the depth of the accelerating gap (Brüche & Scherzer; sect. III.8 of reference). The first slit of the spectrometer, constituting the boundary of this field, will—with respect to tracks in the median plane—act as a divergent lens (Davidsson & Calbicks) the focal distance of which is $2d$. The result is, that these ion tracks enter the analyser with angle 2θ to the axis. The median plane aperture of the focusing system is limited to $2\theta_0$ by the circular stops of the analyser. The fraction intercepted by these stops is then:

$$1-\eta=\exp\left(-\theta_0^2 e\,U/4\,k\,T\right). \qquad \text{(III.1).}$$

Inserting relevant figures—$U = 1000$ V, $T = 1000$°K, $\theta_0 = 0.04$—gives: $1-\eta = \exp(-(100\theta_0)^2) = 0.01$; the angular half-height width of the beam being abt. 0.01 radians within the first slit. With $U = 500$ V, the result is: $1-\eta = \exp(-(70\theta_0)^2) = 0.1$, the angular beam width being increased to 0.014 rad.

As to the divergence experienced by the ion tracks at right angles with the median plane, where no refocusing occurs, the fraction collected is determined by the length of the stop placed just ahead of the mass-selecting collector slit (referred to as the selector slit), and by U/T. This aperture being about 0.012 rad, $1-\eta = 0.2$ and 0.45 resp., at the voltages U considered; the entrance slit is not active as a lens in this projection. Direct measurement of the angular width of the beam (exp. I6) yielded, in fact, a total half-height width of 0.036 rad (1150 V accelerating voltage). The excess spread is probably caused by curvature of the filament or the like.

Thus a considerable fraction of the ions entering the analyser are always prevented from reaching the collector, and the conditions of measurement must be arranged so as to make this fraction independent of mass, if mass discrimination is to be avoided. Evidently, the accelerating voltage, U, must be kept fixed, and the mass sweep obtained through varying the magnetic field (cf. Sect. III.2 D); but one has to make sure, also, that the ion beam as a whole is kept fixed and not displaced by electrodynamic forces on the ion source, or by some change of field geometry. The effects of such displacement are reduced, if the beam is always centered correctly; this was done by adjusting the beam direction for maximum collector current by means of the three controls afforded by the beam director (Sect. II.2). However, experimental investigations and theoretical considerations are necessary in order to ascertain to what extent the ideal conditions are approximated.

Since the measurements reported in this paper were made during development of the apparatus, the conditions were not the same in all experiments. In order to indicate the state of the apparatus at the time of the experiments, these were given a systematic notation (e.g. D1, D2, D3, ...); the key to this follows here: (D) the oldest measurements, in which relative abundance ratios, only, were sought, a filamentary anode and a plane collector being used, and the spectrum scanned by varying the ion energy; (G) measurements of initial ratio on powdered rock; (H) experiments with atomic beam ion sources, using filamentary or indirectly heated anode; (I) experiments with residues of solutions on filamentary anode, with the specific object of attaining the integral ratio; (J) measurement of initial ratio of such residues, a cage collector being substituted for the old one; (K) similar measurements, using the vacuum lock for the ion source; (M) measurements on pure salt solution residues in connection with electromigration experiments (Lundén *et al.*).

III.2. Erratic mass discrimination of ion source

The fractionation inherent in the emission of isotopic ions being part of the object of this work, effects due to source geometry etc. are treated as instrument errors. The following have been investigated.

A. Space-charge limitation of the emission

In order to extract the temperature-saturated emission current of density j, the minimum accelerating voltage, U, to be applied on the plane parallel electrodes at the distance d, is given by:

$$U^{3/2} = 16.35\, j d^2 \sqrt{M}, \tag{III.2}$$

M being the atomic weight of the ion. Thus, from an area of 4 mm^2, with 500 V on 0.5 cm, the critical current of potassium ions ($M = 39$) is about 500 μA. In practice, the emission usually is less by several orders of magnitude, and perfect thermal saturation is attained.[1]

---

[1] The field at the emitting surface has some influence on the saturated emission; cf. Copley & Phipps, 1935.

B. *The magnetic field of the filament heating current*

The magnetic field of this current is nearly uniform just outside the emitting surface. Applying the well-known formula, $\int H\,ds = 4\pi I$, one obtains $H = 2\pi I/b = H_0$, b being the width of the ribbon filament. The maximum occurring in the present experiments is 50 gauss. At some distance, x, from the surface, the field will fall off as $H = 2I/x$, this formula being applicable when $H < H_0$. The accelerating electric field is nearly uniform over the accelerating gap, $0 < x < D$.

The electric field, the analyzing magnetic field, and the considered small perturbating field act in three perpendicular directions; thus the deflection, θ, due to the last-named, is easily worked out in an elementary way, with the result:

$$\theta = [(H_0 b/\pi)/(H R)](1 + \ln \pi D/b). \tag{III.3}$$

Here H and R are the field strength and radius of curvature of the ion path in the analysing field. With $R = 8$ cm and $H = 2$ kG (a case more unfavourable than those met in the present work), θ becomes: $(1 + 2.8) \times 10^{-4}$ rad. This small effect must be considered practically harmless to abundance ratio determination.

C. *Electrodynamic effects on the ion source geometry*

These are particularly important in the present spectrometer, where filamentary anodes are placed in a field of 2 to 3 kG. It may be doubted whether the Mo springs are sufficiently strong for straightening the filament even when heated. The direction of the beam often changes when the temperature is increased; mostly, however, irreversibly, as a result of local changes in the emissivity of the surface, but, perhaps, sometimes due to change of the shape of the filament; vice versa then, the changes in magnetic field strength for mass scanning might cause such changes in filament geometry. Several filaments, of varying rigidity, have been used, but no large effects on the abundance ratio measured were obtained.

The ratio ^{39}K : ^{41}K, in several samples, was measured in 26 experiments with three filaments (11 with *fil. I*, 12 with *fil. II*, and 3 with *fil. III*); 9 differences in ratio were obtained for comparison (viz. six (*fil. I*) – (*fil. II*), two (*fil. II*) – (*fil. III*), and one (*fil. I*) – (*fil. III*); the means of which are:

(*fil. I*) – (*fil. II*)	(*fil. II*) – (*fil. III*)	(*fil. I*) – (*fil. III*)
0.03 ± 20 %	− 0.25 ± 20 %	0.32 ± 25 %

If measures obtained by the different filaments are treated as equivalent, the probable error thus introduced, ± 0.20 %, is within the limits of error of measurement.

The deformation of the filament due to the analysing magnetic field is expected to be different with a.c. and d.c. (rectified, although not filtered). Experiments performed gave the following result on the ratio ^{39}K/^{41}K:

$$\text{(a.c.)} - \text{(d.c.)} = -0.10 \pm 10\,\%.$$

Measurements with the indirectly heated anode, which should be free from the effects considered, have given results a little different from those of an ordinary filament, viz. 14.29 ± 1 (exp. H4) against 14.33 ± 1 (exp. H2), in the case of an atomic beam of K, a wide selector slit, and 1100 V accelerating voltage (see Sect. IV.4). This result would then lead to a correction of −0.3 % to the ratio of ^{39}K to ^{41}K, when measured with a filamentary anode; the probable error of this correction being not less than 0.3 %.

D. Electric mass sweep

If scanning is carried out by varying the accelerating voltage, discrimination is introduced mainly through the lack of focusing in the direction of the magnetic flux, because the beam spread is greater than the length of the limiting stop (cf. Sect. III.1). Direct measurement (exp. G8) in the interval 500–1500 V yielded the relation: $I_{\text{coll}} \sim U^{0.5}$, which is in formal agreement with eq. (III.1). Strangely enough, an analogous relation proved valid also for that part of the emission current which is intercepted by the first slit jaws. The effect is probably due to influence of the accelerating field intensity on the saturated emission.

Whereas the issue of this experiment does not preclude interaction of the magnetic field with the anode geometry, it does certainly display the great discrimination introduced by electric mass scanning.

E. Influence of field intensities on abundance ratio

The integral effect of all influences from the electric and magnetic field intensities is studied directly by measuring the ratio at different accelerating voltages. Measurements performed at different times manifest small trends of ratio with accelerating voltage, but of varying sign. Exp. I4, being the most accurate one, has given the following result on the ratio of ^{39}K to ^{41}K:

Ion energy, eV	790	1145	1465
Ratio, % difference from arbitrary mean	−0.050 ± 45	± 0.000 ± 20	+ 0.075 ± 30

The trend reflects effects of variations in electron release, in reflection of ions at the collector, in beam width and masking effects, magnetic saturation of the pole pieces, etc. There is no sure indication as to the sense and manner in which extrapolation would eliminate these influences, and it is probable that the operation in a medium voltage range would be most nearly ideal.

III.3. Influence of beam direction

The ion source anomalies just considered, acquire importance chiefly through the effects of varying beam direction at the first slit. These phenomena have been investigated directly. Preliminary measurements had indicated that they were rather small. In order to make out their character, and possibly state their trends in ordinary spectrometer operation, the precision peak height ratiometer (R II) was constructed, making possible measurements to better than 0.1 % under good conditions. The following results were obtained with filamentary sources at about 1100 V and using a wide selector slit.

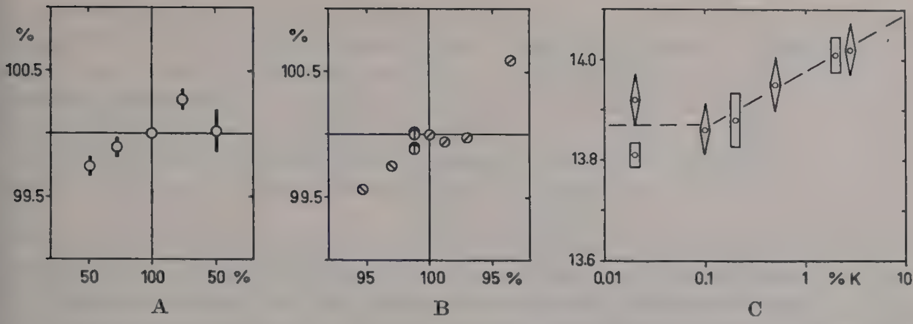

Fig. 10. Discriminating effects. *A*, due to beam translation relative to the entrance slit; *B*, due to beam inclination in the median plane of the magnetic field; *C*, due to varying thickness of coating on filament, in terms of concentration of sample solution: rectangels for exps. I9–I11, I13–I16, rhombs for exps. M26–M29. The ordinate represents the ratio $^{39}K/^{41}K$.

A. Beam translation across the first slit (exp. I2).

The diagram of Fig. 10A gives the relative variation of the abundance ratio, $^{39}K:^{41}K$, obtained by a filament covered with powdered leucite. As there was no scale on the knob of the beam directing device, the movement of the ion source was measured by the ensuing reduction in the ion current which passes the slit. The trend of the variations is not quite regular, and these should be regarded as due to local differences of the emitting surface. On account of the absence of focusing at the ion source, different parts of the surface are measured at different beam positions. It is a general experience, that an abrupt change in the ratio can occur when the ion source, in the course of a protracted experiment, has spontaneously become untrimmed and has been reset by a small adjustment of the beam position. In the case of exp. I2, these changes evidently were about ± 0.25 %. This variation, then, is probably related to the variations experienced in measurements made on the same sample but at different days. These variations are invariably much larger (≈ 0.4 %) than those experienced during a single run (≈ 0.1 %).

B. Beam angle to the median plane (exp. I6)

The influence of this angle was studied by tilting the ion source (Fig. 3A, screw *8*). The screw head carried scale divisions which define the tilting angle. The ions, being accelerated in the quasi-uniform field between the tilted source and the fixed entrance slit, acquire $\frac{2}{3}$ of the tilting angle. A slight symmetric increase of the ratio with increasing angle (about 0.5 % for the half-height angle, 0.18 rad) was discerned, which implies that the spread of the beam was smaller for the heavier isotope. Numerical evaluation of the data yields a correction, $+0.25 \pm 15$ % to the zero angle value, which was 13.86. Other measurements of this kind have given no definite decision as to the sign of the effect, which in this experiment was the opposite of the one reported in Sect. III.2 C.

C. Beam direction in the median plane (exp. I4)

The angle of direction could be assessed only by referring to the subjective impression of the ion source tilting angle, and the reduction of beam intensity occurring when the beam becomes oblique enough to suffer reduction in intensity by the internal stops. In the diagram, Fig. 10B, the ratio is plotted against the relative beam intensity, the diameters drawn into the circles visualizing the direction of the tilting angle by referring to the projection of Fig. 2. As to be expected, there is little discrimination in the region of slight loss of intensity; at more than 2 % loss, however, discrimination starts at a rate of 0.1 % per % of intensity reduction. This signifies that the positions of the isotopic beams are not identical at the respective moments of measurements, as they should be in the case of magnetic mass scanning. The heavier isotope, on the average, has a more periferal position.

Mass discrimination will, accordingly, occur when a considerable fraction of the beam current in the median plane is intercepted by the stops. In the range of ion energies adopted for routine, by proper trimming of the ion source, it will be achieved that the ion optics of the median plane do not introduce any discrimination. With voltages less than 750 V, there will be no latitude of trimming, and such discrimination (amounting to the order of 1 %) could be not ruled out. The cause of the discrimination is not known, but a variable non-uniformity of the magnetic field is the most probable one.

III.4. Collector efficiency

The ion current measurements may be falsified by electron release and reflexion of ions. These effects depend on the geometry of the collector and appertaining slits. At the construction of the spectrometer, no regard was paid to the possibility of reflexion of ions, and the collector was given the shape of a plate. Recently a hollow collector of the shape depicted in Fig. 2, *13*, was used, thus affording a check on the earlier measurements.

A. Electron release

The electron current released from the collector plate was less than 2 % (exp. G5; K^+ at 1150 V). The effect on the ratio, $^{39}K/^{41}K$, was less than 0.15 %. This is in accord with measurements by Inghram, 1946, and Ploch & Walcher, 1952. Within the range of accelerating voltages used, the electron release does not vary more than proportional to (ion mass)$^{-1}$; for a 5 % mass difference, the correction to the ratio named is about -0.1 %.

B. Ions reflected at collector plate

A more serious problem is presented by the reflected ions, because of the, sometimes strong, dependence on ion mass (Ploch, 1951). The total yield of reflected ions should be rather low, however, as the collector plate was never baked out. Ploch (l.c.) found for Li^+ on Cu, at 1200 V, an isotopic difference of 1.15 %; for Li^+ on Pt, at 2000 V, 1.7 %. For K^+ this effect is one order of magnitude less. The sign of the error is such as to reduce the yield of the lighter isotope.

C. Comparison of plate and cage type of collector

A direct determination of the total error due to electron release and ion reflexion (which act in opposition in the error of measurement) is afforded by a comparison between the results on the ratio of ^{39}K to ^{41}K in the evaporation residue of phosphate solutions of different concentrations; the results were obtained both with plate collector (exps. I9–11, I13–16) and with cage collector (exps. M26–29). The mean systematic difference is $-0.3 \pm 2\,\%$, the plane collector giving preference to the heavier isotope.

III.5. Defocusing effects

A. Vacuum effects

Investigations on the stopping and scattering of slow ions (Sherwin; cf. Cook) have established effects which are too small to give appreciable errors in usual conditions of spectrometer operation. Measurements with the present instrument (exp. I5) indicate a maximum correction, $-0.1\,\%$, to the ratio of ^{39}K to ^{41}K (at 1150 V, and with wide collector slit) at a vacuum of 3 μTorr. No reason was ever found to ascribe variations in abundance ratio measured, to vacuum conditions. Of course, gas broadens the peaks at their bases, and it becomes necessary to check the spectrum for the continuous background.

B. Space-charge defocusing

In most analytical mass spectrometer work, the beam intensities are so low that the focusing at the selector slit is not appreciably affected. This is easily checked by direct measurement of abundance ratio at different source emissions. With the atomic-beam surface-ionization ion source, very reproducible ratio measurements are possible. The results (exps. H2, H7) indicate that from 10^{-11} to 10^{-8} A of main isotope current, i_{39}, the ratio does not change as much as 0.1 %.

This issue agrees with a theoretical calculation of the effects of space-charge on focusing and collector current intensity. In Appendix 1, the following formulas are derived; they give corrections to the ratio measured, which are due, on one hand, $\Delta\lambda_1$, to a change in the condition of focusing in the magnetic field, on the other, $\Delta\lambda_2$, to an increase of the beam "height" (width in the direction of the magnetic flux):

$$\Delta\lambda_1 = \frac{1}{2} C_1 M \gamma; \quad \Delta\lambda_2 \leq \frac{1}{4} \pi^2 C_2 (a/y)\, \gamma; \quad \gamma = \frac{\pi m c^2 I}{B e U h} \text{ e.m.u.} \qquad \text{(III.4)}$$

Here a = radius of ion path in the magnetic flux density, B; I, ion current of the main isotope; e, charge, m, mass, eU energy of the ions; h, mean height, $2y$, mean width of the beam; M, geometric mass resolution; c = velocity of light; C_1 and C_2 are correction factors less than 1, which are estimated from the shape, $h{:}2y$, of the average cross-section of the beam. The correction $\Delta\lambda_1$ only applies to the case, that entrance and selector slits have equal widths, viz. a/M. With a wider selector slit, this kind of space-charge effect vanishes, practically.

Two instances of particular interest to the present work will here be considered numerically.

(1) *The determination of the abundance of* ^{40}K.—In this case measurements were made with narrow selector slit, of width 0.3 mm. With $a = 80$ mm, $M = 270$. Maximum current I was 10^{-10} (e.m.u.). Other data are: $m/e = 4.14 \times 10^{-3}$, $B = 4000$, $U = 1.3 \times 10^{11}$, $c = 3 \times 10^{10}$, $y = 0.1$, $h = 0.6$. From this, $C_1 = 1$, $\gamma = 3.75 \times 10^{-6}$ and $\Delta\lambda_1 = 0.05\,\%$.

In order to calculate $\Delta\lambda_2$, C_2 is to be estimated for $h/2y = 3$. One obtains about $\frac{1}{2}$; thence $\Delta\lambda_2 = 0.03\,\%$. Thus, the total error in the ratio of ^{39}K to ^{40}K becomes less than 0.1 %, and may be neglected.

(2) *The determination of the ratio of ^{39}K to ^{41}K.*—The selector slit being much wider than the first slit, the space-charge focusing error, $\Delta\lambda_1$, is absent. In some measurements, however, $\Delta\lambda_2$ acquired some importance, since currents, I, of 10^{-9} e.m.u. were employed. Other data being about the same as in the first case, one obtains: $\Delta\lambda_2 \leq 0.3\,\%$.

Such large currents occurred only in the integrating measurements on residues of 2 % potassium phosphate solutions. The accuracy of the measurements referred to (exps. I9–10) was not sufficient to make any such effect noticeable. Due to 75 % of the K^+ being collected at this high current intensity, a correction of $0.1 \pm 1\,\%$, at most, might be applied to the mean abundance ratio obtained. In fact, the much more accurate measurements of exp. H7 do not display any space-charge effect.

C. *Magnetic flux saturation*

Since ion source and collector are situated close to the magnet gap, the stray field will only slightly affect the position of the focus; if only the gap field is uniform, there can arise no dependence on ion mass. In sector field, however, mass discrimination in focusing may become important (Becker & Walcher), the effect being similar to that of space-charge. With duly flat peak tops, it should always be negligible.

III.6. Survey of corrections and limits of error

From the preceding investigations it follows that the construction of spectrometer and ion source exerts an influence, amounting to a few tenths of a per cent of the ratio measured. It appears probable that these effects vary from one experiment to another, or during the course of an experiment, but it has, for practical reasons, not been possible to perform all necessary checks in every experiment. Thus the discriminating effects found will provide sources of variable errors, rather than definite corrections to the measurements. The following is the result of weighing the data presented in this chapter.

Percentage correction and probable error due to

filament deformation (III.2C, III.3B)	0.00 ± 30;
filament adjustment (III.3A)	0.00 ± 25;
plane collector influence (III.4C)	$+0.30 \pm 20$;
vacuum influence (III.5A)	-0.05 ± 05.

IV. Measurements of initial ratio, $^{39}K/^{41}K$

IV.I. Powdered leucite on filament

A. Procedure

The analyser was recently gilded; the collector had the shape of a plate. The ion source was prepared by mixing some powdered leucite[1] with water and applying a drop to the filament, finally heating the filament in air transitorily to redness. In the present experiment, the coating had already been used for some time; however no indications of exhaustion are visible in the records. After trimming the ion source, the peaks were flat-topped with a slope less than 0.25 % on a width of 0.15 MU, which represents the influence of the accelerating voltage on emission (Sect. III.2 D).

B. Measurements (exp. G8)

The variation of isotope current, i_{39}, and the current to the entrance slit jaws, i_{em}, with accelerating voltage and magnetic field density was measured; the results have been discussed in Sect. III.2 D. Further, the ratio $^{39}K/^{41}K$, was measured under variation of the accelerating voltage; these data are assembled in Table 2.

The measurements were obtained by reading the panel instrument of the collector current amplifier. The readings on the two peaks were taken in regular succession: 39, 41, 41, 39, 39, 41, etc., with one reading every 15th second. The exchange of peaks was carried out by switching in the magnet current circuit; but the maximum reading was obtained by a slow variation of the accelerating voltage. The magnet current had to be adjusted before each series of readings so that the maximum readings were obtained at equal voltages, in order to eliminate the influence of a variable accelerating voltage. In some cases, these voltages were read, and their difference, Δu_I, employed for correcting the ratio measured according to Sect. III.2 D.

Table 2. Measurements on powdered leucite. Filamentary anode. Exp. G8.

Date	Ion energy eV	i_{39} μμA	i_{em} μμA	q	Date	Ion energy eV	i_{39} μμA	i_{em} μμA	Δu_I MU	q
8/9	1100	86	80	14.29±5	10/9	1200	87	660		14.27± 3
	500	57		14.21±4		900	77	580		14.25± 6
	1430	94	88	14.30±6		690	66	520	+0.05	14.21± 7
						540	56	460	±0.00	14.15± 3
9/9	1140	72	620	14.28±4		720	68	540	−0.06	14.12± 4
	820	62	540	14.18±4		930	78	600	−0.05	14.38±10
	540	48	450	14.21±3		1185	87	678	−0.18	14.40±12
	870	62	540	14.15±3		1470	96	760	−0.08	14.17± 5
	1170	71	630	14.30±4		1200	89	680	+0.04	14.23± 6
	1440	77	700	14.35±4						
	1170	69	600	14.30±3						

i_{39} = separated current of isotope 39; i_{em} = current collected at the entrance slit; Δu_I = difference of ion energy of isotopes in equivalent atomic mass units; q = ratio of $^{39}K/^{41}K$, ± linear average of deviations of 7 individual measurements.

---

[1] Vesuvius; the sample obtained from the collections of the Mineralogical-Geological Institution, Uppsala.

Sixteen readings make one series. The readings had to be corrected for continuous background (read before and after each series, at 39.5 and 41.5 MU), and for meter division error. Then the ratio was calculated for every pair of readings, two consecutive pairs being used for calculating a mean value; from the 16 readings, 7 means are obtained. The median of these means, and the average deviation of the 7 means, are entered into the Table 2, after correcting for amplifier range errors.

C. Results

The general means for the three days of measurement are: 14.27 ± 2; 14.24 ± 2; 14.25 ± 2. Numerical analysis makes a trend with accelerating voltage probable, amounting to about 0.10 per kV. The various possible causes of such variations have been discussed in Ch. III; since no particular method of extrapolation is indicated, rather wide limits of error have to be assigned to the result, e.g., $^{39}K/^{41}K = 14.25 \pm 10$. This agrees with Brewers measurements.

D. Comparison with further experiments on powdered rock

A few other determinations on powdered rock are available:

(1) *Orthoclase*: 14.07 ± 3 (exp. G10). The plate collector was used, but the trimming of the ion source was not correct (R II, Sect. III.5C); thus the difference relative to the leucite ratio is not considered significant (cf. Sect. III.3C).

(2) *Leucite*: 14.17 ± 4 (exp. K15). A cage collector was used. This lower value, also, agrees with the measurements of Brewer and Cook.

On the whole, these measurements give 14.20 ± 5 for the ratio in powdered rock, without any corrections for instrumental errors.

IV.2. Phosphate solutions on filament

A. Procedure

The solution was prepared by dissolving KCl in an equivalent quantity of diluted H_3PO_4. One drop of solution was applied to the filament and evaporated to dryness by gentle heating. Immediately before inserting the source into the spectrometer, the coating was heated in air to dark red heat. A clean surface of Pt is water repellent, and it is convenient to use a glass pipette treated with a silicon fluid (Desicote, Beckmann Ltd.), by which means, drops of volume less than 0.25 mm³ may be obtained. In case the concentration is only 0.01 % in KCl, the quantity of sample in the drop is only 0.025 μg, which is enough for an analysis. Filaments which had been coated with samples containing fluoric acid obtained a surface which easily accepted water; on such filaments the drops are larger.

Before coating, it is necessary to remove the residue of the preceding sample. Heating in vacuum was not alone sufficient, without taking the risk of melting the filament; thus the main part of the sample was dissolved by leaching with steam for ½ hour before vacuum-heating at 1400°C.

B. Experiments I9–11, 13–16

The filament and collector were the same as in the experiment related in Sect. IV.1. The ratio, however, was measured by the peak height ratiometer (R II, Ch. III).

The results are displayed in the diagram, Fig. 10C. The heights of the rectangles indicate the probable errors of the abundance ratios. It will be noted, that the ratio $^{39}K/^{41}K$, in these experiments is more than 1 % lower than that obtained for powdered leucite in the same circumstances.

C. Experiments M26–29. Discussion of results

The method of measurement was that of Taylor (R II, Sect. III.7); the cage collector was used. These results are, also, illustrated by the diagram, Fig. 10C, the heights of the rhombs indicating the probable errors. The difference to the "I" measurements is considered representative of the effects of change of collector geometry, and is evaluated in this respect in Sect. III.4C.

Evidently, there is a considerable influence of the thickness of the coating on the ratio measured. Since it cannot be expected that the ratio will decrease infinitely with decreasing coating thickness, it appears reasonable to conclude, that concentrations less than 0.1 % give a practically limiting value of the ratio. Whether or not this value is correct, it seems favourable to employ thus diluted solutions for determining relative isotopic abundance ratio. From the diagram, the standard value, 13.87, is obtained. However, taking into account the systematic error of -0.04 in the "I" measurements (Sect. III.4C), 13.89 appears a good mean for the standard value. Applying relevant corrections according to Sect. III.6, there results, 13.88 ± 7. The results obtained on powdered rock, 14.20, fit well with the trend displayed by the measurements on solution residues, since the powder makes a very thick coating.

IV.3. Solutions of natural samples

A. Methods of sample preparation

Most substances containing potassium, as minerals, salts, plant ashes, give off potassium ions on heating in contact with platinum, particularly if phosphoric or silicic acid are added; these are to bind the K in less volatile compounds, in order to prevent loss of this element in un-ionized form at low temperatures. It has thus become a practice to prepare the hot ion source in this way (or in a corresponding one for impregnating the platinum with potassium). The mass spectrum obtained is practically free from peaks due to other constituents, because K is more easily ionized than any other element, the rare alkali metals, Rb and Cs, excepted. The composition of the samples, also, remains unaffected by uncontrolled isotope-discriminating processes possibly associated with any chemical purification. The simplicity of this technique allowed Brewer to carry out a broad survey on natural variations of the isotopic abundance (1936b).

The detection of the effect of coating thickness in the preceding investigations then led to a repetition of some of Brewers measurements with the alteration, that chemical decomposition of insoluble substances, and some separation of potassium salt, were carried out by methods drawn from quantitative chemical analysis (Kolthoff & Sandell)—applied however, with some simplification, after the examples given by Brewer (1936c) and Cook. The solutions obtained, then, contain other elements too, as Ca, and are not quite equivalent to the pure solutions referred to in the preceding sections.

Table 3. Results $^{39}K/^{41}K$ on solutions of some natural samples.

Sample Concn. of soln.	Exp. no.	Individual determinations	Means	
(1)	J4	(14.09 14.06) 14.04 14.04	14.04	13.97 ± 2
Leucite-HF	J6	(13.74 13.80 13.84 13.84) 13.95	13.95	
0.12 % K	K1	13.97 14.02	14.00	
	K2	13.95	13.95	
	K6	13.97 13.91	13.94	
(2)	J2	(13.91) 13.98 13.93	13.96	14.07 ± 4
Sea water	K13	(14.02 14.00) 14.11 14.11 14.06 14.17	14.11	
0.05 % K	K16	(14.04 13.96 14.04) 14.08 14.13 14.16 14.13 14.15	14.14	
(3 a)	J7	(13.51 13.26 13.62) 13.52	13.52	13.68 ± 8
Kelp ashes	K3	13.48	13.48	
water-extract	K18	13.96	13.96	
0.4 % ashes	K19	(13.76 13.68 13.62) 13.79 13.74	13.76	
(3 b)	K12	14.00 13.98 14.00 14.01	14.00	13.95 ± 3
Kelp ashes	K14	13.88 13.83 13.92 13.93 13.93 13.94 13.94	13.90	
$HClO_4$-extract	K20	14.04 14.06 14.04	14.05	
0.4 % ashes	K21	(13.87) 13.81 13.83 13.85 13.91	13.85	

The ratios are not corrected for mass discrimination of the spectrometer. The corrected values are, according to Sect. III.6, lower by 0.01.

B. Measurements

The procedure was that described in Sect. IV.2. The substances investigated were: (1) leucite dissolved by HF; (2) sea water, K separated by $HClO_4$; (3) a Pacific kelp, Macrocystis pyrifera[1], which, after rinsing thoroughly with water, was ashed; the ashes were partly (sample 3a) leached with water, and partly (sample 3b) treated for separation of K as a salt.

The measurements started with only 10^{-11} A current i_{39}, and continued with 10^{-10} A. The results indicate, in several instances, a systematic difference between the determinations made at different current intensities, the early measurements appearing less representative. These are not used for the comparison of different samples, and are entered within brackets in the Table 3, which gives an assembly of all determinations on the samples mentioned. The solutions contained about 0.1 % K; such thin coatings aging rapidly, only a few determinations were obtained in some experiments before signs of exhaustion became noticeable. In general, only the data obtained within the first 0.1 μAs of $^{39}K^+$ collected, are considered significant.

C. Comments on the results

The p.e., or median deviation, of the ratio determined by a single experiment is about 0.4 %, except for those on sample 3a, the water extract of the kelp ashes, in which case it amounts to at least 1 %. However, the mean ratio obtained for this sample differs by about 2 % from that of leucite or sea water, and this result must be considered unlikely to be due to a random error. So far, these measurements confirm the result obtained by Brewer (1936 b), who found extremely low ratios in this sea-weed. Strangely enough, this difference disappears when the kelp ashes are treated chemically in order to isolate a potassium salt; there is no sign of the kelp potassium having an abnormal isotopic constitution.

---

[1] Collected abt. 1900 at San Francisco; the author is indebted to Dr. Rolf Santesson for supplying this sample from the herbarium of the Institution of Systematic Botany, Uppsala.

The conclusion to be drawn out of these facts is that general admixtures to a sample solution may affect the outcome of the isotopic abundance measurement, when using a coated filament as a hot anode. It is plausible, that variations in crystal structure influence diffusion processes, on which depend the mass discrimination in thermionic emission, or evaporation. Thus, any ratio down to the integral value (about 13.6, according to the measurements to be described in the following chapter) could be expected to appear as the initial ratio. It seems probable, also, that the same effect is active in the process of impregnating the filament in the experiments of Brewer, since both types of hot anode give practically the same abundance ratio. However, the very low ratio, 12.6, found by Brewer in some kelp, cannot be accounted for in this way. Also, Brewer in some cases (1936 c) checked the chemical treatment for selectivity, with a negative result, although it is not quite clear if the possibility of samples having an individual behaviour in this respect, was completely ruled out. The nature of the process leading to an isotope enrichment of more than 10 % in a living organism, is still quite obscure.

The sea water (sample taken in the Bothnian Sea) has given a rather high ratio, differing to the rock sample 1 by 0.7 %. Calling into attention the fact that the solutions analysed were not really chemically pure, such a difference might well be ascribed to source fractionation. Measurements on commercial KCl (exps. M26–29), made with the same filaments in the same time interval as those presented in this section, have given a low value, about 13.90, for potassium concentrations below 0.2 %. Experiments with addition of $CaSO_4$ to the sample solution 3b, in fact, gave as the result an increase of the ratio by 1 %. Another instance of such irregular discrimination might be provided by the analysis of samples which differ greatly in magnitude (Lundén *et al.*); the large reference sample gave 13.94 ± 2, while interpolation from the values for the 10 mg samples from the diffusion column, would indicate 14.05 ± 2. Similar effects are reported by Collins & Rourke concerning Li.

Regarding all this evidence, it appears safe to say that only coatings of pure salts, of defined chemical composition, should be used for abundance determinations in potassium. The initial ratio obtained may be used for studies of *variations* of isotopic abundances, but not as indicating the true, absolute composition. In order to establish this, experiments with integrating the ion currents were started and will be reported in the next chapter.

IV.4. Experiments with the atomic-beam ion source

These were intended to eliminate, at one time, the inconsistencies met with in the ion emission from anode coatings, and the risks of deformation of the anode due to the magnetic field. Because of the difficulty of directing a beam of a less volatile compound of potassium onto the anode surface without interfering with the uniform-field geometry, the metal itself had to be used. Because of various circumstances, the experiments gave little conclusive evidence, and will here be related in short, only.

The experimental arrangement was described in Sect. II.2. Potassium metal (Merck) was extruded into a wire of 1 mm diameter; a piece of 1 to 2 mm length was introduced into the crucible under xylol. The crucible was quickly transferred to the spectrometer, which then was evacuated slowly, to prevent dislocation of the sample by violent boiling of the xylol.

Filament anode (exps. H1–2)

The crucible was heated by current from a storage battery; 0.13 W were necessary for obtaining 10^{-9} A current, i_{39}. The filament temperature was abt. 1350°C. At first, a ratio 14.27 was measured. The next day, the ratio started at 14.33 and remained there within ± 0.01, independent of changes of filament temperature and ion current, i_{39}, within the range 10^{-11} to 10^{-9} A. Only transiently with the changes of conditions, there occurred deviations to 14.28 and 14.50, in the extremes. The variations are explained by assuming re-evaporation of potassium from various surfaces in the spectrometer, in particular, from the focusing electrode of the ion source and the slit jaws.

Equipotential anode (exp. H4)

Measurements during 6 consecutive days always gave the ratio 14.29 within ± 0.01, when stationary conditions had been achieved (anode temperature about 750°C). This takes a rather long time, since the heating of the entrance slit jaws by radiation from the anode was stronger than in the case of a filament anode. Since the crucible was surrounded by a shield connected to the slit jaws, and these were insulated from the spectrometer body by mica foil, their temperature gradually rose and made it necessary to reduce the heating power (to 0.03 W for 10^{-9} A of i_{39}). Again, during the heating or cooling of the oven, deviations were obtained in the same direction as in the exps. H1–2. During degassing of the anode, before heating of the oven, low values, applying to absorbed potassium re-evaporating from the anode, and averaging abt. 14.10, were measured.

Summary

Several selective effects evidently add up in these experiments, and make the interpretation of the results uncertain. The differences between the ratios obtained by the filamentary and equipotential anodes is accepted as indicating an effect of variation in the shape of the filament (Sect. III.2C); however, it is difficult to assess the accuracy of this determination.

V. Measurement of the integral ratio, $^{39}K/^{41}K$

V.1. Theory of fractionating evaporation

When a rarefied gas flows into a vacuum through an aperture which is small in comparison with the mean free path of molecular diffusion, the number of molecules lost per unit time is proportional to the inverse of the square root of the molecular weight. The same may be supposed to hold in some cases of evaporation of a substance from the surface of a solid. In such cases, the variation of isotopic composition with increasing exhaustion of the sample is calculated as follows.

Let $n(t)$ and $m(t)$ be the number of isotopic molecules of masses, N and M, which remain at time t, and q the ratio of the numbers of molecules N and M, which are evaporated per unit time, at time t: $q = q(t) = (dn/dt)/(dm/dt)$. The mentioned relationship between molecular weight and rate of evaporation yields:

$$n(t) = n(0)e^{-tf/\sqrt{N}};\ m(t) = m(0)e^{-tf/\sqrt{M}},$$

f depending on the temperature and the conditions of the surface, but supposed to be fixed during the evaporation. Denoting $n(0)/m(0)$ by Q, i.e., the integral ratio, one obtains

$$q = \sqrt{M/N}\,Q\,e^{-tf(1/\sqrt{N}-1/\sqrt{M})} = \sqrt{M/N}\,Q\,(n(0)/n(t))^{\sqrt{N/M}-1}.$$

The initially measured ratio is $q(0) = \sqrt{M/N}\,Q$. Introducing $\alpha = \sqrt{N/M} - 1$, the result is condensed into

$$q/q(0) = (n(0)/n(t))^{\alpha}. \tag{V.1}$$

In the diagram, Fig. 11B, the typical course of $q/q(0)$, according to this equation, is displayed for the case, $\alpha = 1/61$.

In most cases, $\alpha \ll 1$. Thus, approximately,

$$\alpha \approx \tfrac{1}{2}(N - M)/M \tag{V.2}$$

and

$$Q \approx q(0)(1 + \alpha). \tag{V.3}$$

From the graphic representation of eq. (V.1), the value of α is then read approximately, at $n(0)/n(t) = e$ (the base of natural logarithms); i.e., Q is given by q when 63 % of the sample has evaporated.

V.2. Atomic beam and indirectly heated anode

This ion source was expected to be particularly suited for integral measurements, because of the better source geometry and because of the accuracy obtained in measuring variations of the abundance ratio, a consequence of the slow variations in emission. Difficulties arise, however, in administering a sufficiently small sample of metallic potassium to the crucible, and the experiment (H.7) had to be extended

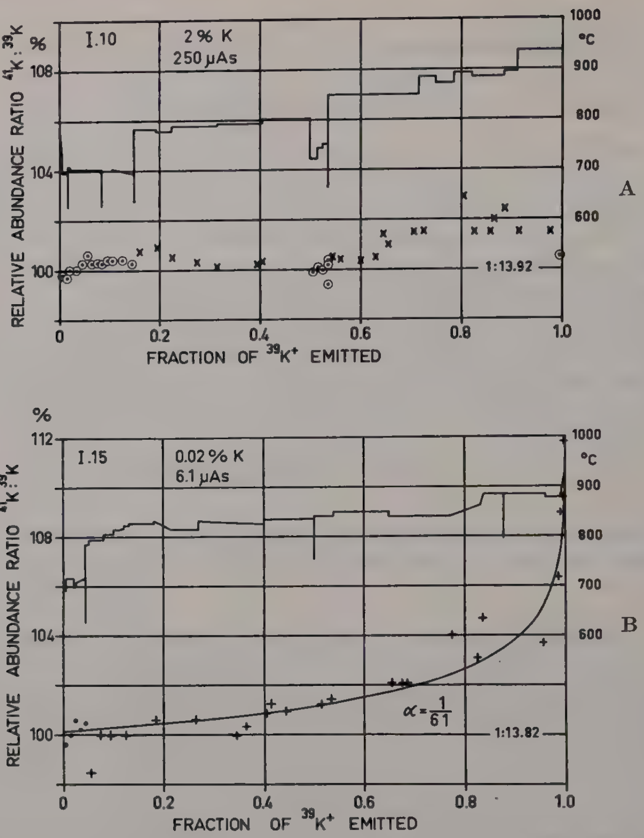

Fig. 11. Variation of isotope ratio during consumption of the ion source. Filamentary anode coated with residue of one drop of phosphate solution of potassium content indicated. Current of $^{39}K^+$ at measurement: • 10^{-11}, + 10^{-10}, ⊙ 10^{-9}, × 10^{-8} A. The total charge of $^{39}K^+$ collected is given in μAs. Broken line and right-hand scale: variation of filament temperature; vertical pips indicate night-time shut-offs.

through 5 days, with ensuing risks of losing part of the sample through oxidation and evaporation during off-operation time.

For the first 70 % of charge, $^{39}K^+$, collected, the ratio obtained was 14.38, with an average individual deviation of ± 0.08 %. The rather large difference from the value, 14.29, of the previous exp. H4 may be the result of faulty ion source trimming (Sect. III.3C), since the proper adjustment of this anode was difficult to check (it was not changed during the course of exp. H7). During the last 25 % of charge collected, the ratio decreased somewhat irregularly, finishing at 13.85. This decrease was associated with the first signs of exhaustion of the crucible.

Potassium has a melting point of 62°C, and is fluid at the operating conditions; the vapour is likely to emerge with an ideal discrimination of 2.5 %, favouring the lighter isotope. However the theoretical curve for $\alpha = 2.5$ is not obtained. Maybe much of the heavier isotope was lost through oxidation etc.

V.3. Potassium phosphate on filamentary anode

The filament was prepared with one drop of solution, which was applied by a slender glass rod. Several concentrations were studied; examples of the results obtained are represented by the diagrams, Fig. 11 A, B. The evaluation has been carried out by two methods:

(1) The points are connected by a polygon line, and the area under the line yields $1/Q$. $q(0)$ was obtained by considering the measurements made during the first 10 % of exhaustion; this initial value of $1/q$ was taken to define the 100 % ordinate.

(2) A theoretical formula (V.1) is matched to the measurements by adjusting the constants, q and α, in order to obtain a minimum sum of squares of errors. Since the determination of $1-x$ is relatively inaccurate for $x > 95\,\%$, such measurements were

Table 4. Measurement of the integral ratio $^{39}K/^{41}K$.

Exp. no.		H7	I9	I10	I14	I15	I16
Solution, % K		(vapour)	2		0.02		
Charge $^{39}K^+$ collected, μAs		315	53	250	2.45	6.1	1.9
Polygon integral method	$q(0)$	14.38	14.08	13.92	13.92	13.82	13.82
			14.00 ± 6		13.85 ± 3		
	Q	14.33	14.02	13.81	13.41	13.56	13.51
			13.91 ± 7		13.49 ± 3		
	α, %	0.32	0.45	0.82	3.65	1.86	2.26
			0.64 ± 12		2.59 ± 37		
Least squares method	$q(0)$				13.90	13.80	13.97
					13.89 ± 3		
	Q				13.46 ± 3	13.58 ± 2	13.49 ± 2
					$13.51 \pm 2_5$		
	α, %				3.17	1.64	3.45
					2.75 ± 38		
Mean values	$q(0)$				$13.87 \pm 3_5$		
	Q				13.50 ± 3		
	α, %				2.7 ± 4		

Note.—The probable error limits given for the individual values of Q, according to the least-squares method, indicate the accuracy by which the measurements fit theoretical functions of eq. (V.1) with the α values given.

not taken into consideration. In calculating the p.e. of the value Q obtained, the effective number of independent observations was determined by counting the number of changes of error sign (Sect. VI.1).

The results appear in Table 4. The values of Q calculated by the two methods agree within a few tenths of a percent. Between results obtained from solutions of different concentrations, there appear, however, large systematic differences, as regards both Q and α (abt. 3 %, and 2 %); the difference in $q(0)$, 1 %, being much less, though definitely outside the limits of error. The diagrams, too, display a striking difference in behaviour between high and low concentrations, i.e., thick and thin filament preparations.

With thick preparations, the general trend of q with time is quite small, the curves, however, having maxima and minima which cannot be ascribed to measuring errors. No reasonable match is obtained with any theoretical curve. The measurements with thin preparations, on the other hand, display a trend in rather good agreement with theory, and approximate values of α and Q can be read directly from the measurements obtained at $x = 0.63$. Now, of course, there is no reason for expecting any definite value of α, e.g. $\alpha = \frac{1}{2}(M-N)/M = 2.5\,\%$, to occur in the complex diffusion in a salt layer on a metal substrate; but the Q values should be significant of the composition of the sample in bulk, and independent of the sample quantity. The measurements, however, give the opposite result. This dilemma will now be analyzed in some detail.

V.4. Discussion of the results on the integral ratio

A. Completeness of exhaustion

The values of integral ratio of Q obtained from the diagrams are misleading if the curves are not complete; i.e., it is essential that the sample be completely exhausted. This is difficult to assure, if the emission does not end abruptly. The collector current, i_{39}, was kept at a nearly fixed intensity by regulating the filament temperature; for this it was necessary to increase this temperature continually. Approximately 0.1 A increase of filament current, I_f, raised lg i_{39} by 0.6. Defining the emissivity, E, of the source by

$$\lg E = \lg i_{39} - 6 I_f + 30 \qquad \text{(V.4)}$$

(30 being an arbitrary constant), the diagram of Fig. 12 was constructed in order to display the variation of the emissivity with the charge $^{39}\text{K}^+$ collected. It will be noticed: (1) the emissivity E is in a general way a measure of the sample quantity, except for the initial part of the run; the ratio of E in 2 % and 0.02 % samples being about 100; (2) the emissivity decreases abruptly towards the end of the runs, indicating that the remaining quantities of sample could not be more than 1 % when the experiments were broken off. The occasional deviations from a smooth curve are in several instances associated with changes of filament temperature; evidently the coefficients of eq. (V.4) may change with the state of the coating.

B. The yield of ions

The following calculations are made in order to get an estimate of the percentage yield of the potassium as ions.

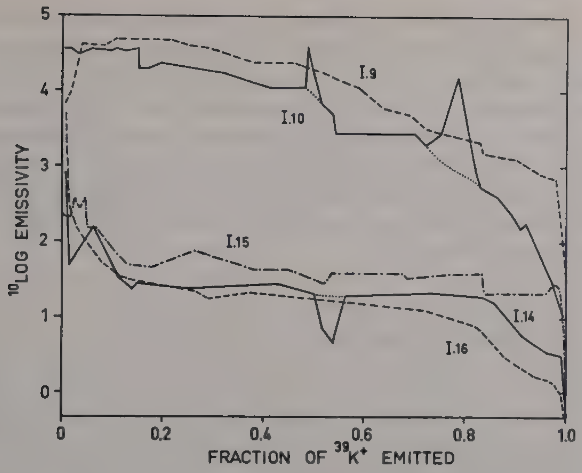

Fig. 12. Variation of the emissivity of coatings during consumption.

In all cases, one drop of solution was applied to the filament. The volume of this drop was estimated at 1 to 4 mm^3, the residue of which was distributed over less than 4 mm^2 of the filament. A 1 % (0.25 M) solution of K thus results in a coating containing 4 to 15 $\times$ 10^{18} atoms per cm^2. The thinnest coatings employed correspond then to at least 100 monomolecular layers (acc. to Sect. I.4). The charge carried by one mole of ions is 10^5 As. Thus the ratio, charge/concentration, of one such drop is 25–100 mAs per % of K. After ionization, a varying fraction of this (10–25 %) is transmitted to the collector. Actually, the "specific charges" measured at the collector range from 0.03 to 0.13 mAs per % in the experiments on thick coatings, and from 0.1 to 0.33 mAs per % in those on thin coatings. The yield of ions is thus estimated at not less than 1 % and not larger than 3 %, and not much different in the two kinds of coatings. From this it follows, that if some loss of sample would occur in the source, e.g. by diffusion through the base metal, the fraction must have been about the same irrespective of coating thickness.

C. Possible causes to the disagreement between thick and thin coatings

(1) The results could be explained by accepting the integral ratio from the thick coatings (corrected for instrumental errors: 13.95; cf. next Section). This is equivalent to saying that the initial ratio in thin coatings (13.92) is free from fractionation. Diffusion and migration in ionic crystal lattices are generally supposed to take place at a rate $\sim M^{-\frac{1}{2}}$; grain boundaries however afford diffusion paths with less selectivity (Chemla & Sue). Also, a coupling between the movements of isotopic ions has to be taken into consideration (Klemm); this would reduce the fractionation in the transport through a crystal lattice. It must, then, be postulated, that the mass selectivity in diffusion within the coating increases with thickness of the latter, attaining the theoretical maximum of $(M_1/M_2)^{\frac{1}{2}}$ in coatings of powdered rock and salts. The α observed in the thin coatings must reflect the fractionation of some process leading to the loss of a major part of the sample on the filament. This loss could be independent of coating thickness and, accordingly, affect the coatings containing a

smaller amount of sample relatively stronger; the selectivity should be just the maximum theoretical one for molecular diffusion. However, as stated under Section B, there is scarcely any margin for such a process. It would be necessary to postulate a higher degree of ionization in the emission from the thin coatings in order to compensate for the loss. The fraction of the emission current intercepted by the entrance slit, becomes smaller towards the end of the runs with the thin coatings; thus, it seems unlikely that any large fraction of the samples would migrate along the filament, since the length of the entrance slit in these experiments was only 5 mm, the filament being 12 mm long.

(2) It is a fact that the abundance ratio also suffers large variations with time in the runs with thick coatings. Upon closer inspection of diagrams such as Fig. 11 B, in several places indications of narrow maxima of $1/q$ become apparent. Simultaneous with this peak, a rapid decrease of intensity was often noticed (which prevented the taking of good readings of the peak value), and sometimes also, a displacement of the center of emission, making necessary a readjustment of the ion source. Furthermore, Fig. 12 indicates that the emissivity, in the case of a thick coating, decreases slowly through the main part of the run, but in the case of a thin one it remains more nearly constant. The interpretation is, then, that in thick coatings there are small domains (crystallites?) which emit better than the environment, and thus become exhausted more rapidly. There develops an increase of $1/q$, which, towards the end, grows so rapidly, that no reading can be obtained with the equipment employed. Other, not exhausted, domains then take over the emission, causing $1/q$ to start anew at a lower value; the filament temperature must be raised in order to sustain the desired level of emission. The thin preparations are more uniform, or comprise only a few domains, and the rate of evaporation is lower; the course of the abundance ratio is more smooth.

If this description of the matter is true, the measurements on thick coatings must give a ratio q too high, because of the method of measurement used (it would have been avoided in a double-beam arrangement with continuous collection of the isotopic ions). The results obtained with thin preparations should be more nearly correct. Naturally, deviations from the ideal course of q must be expected; part of the sample diffuses into the metal base and is re-emitted after temperature rises, in particular near the end of the run; or it is lost altogether by diffusion to the back of the filament. Other experience (Table 3, sample 3a; Table 5, exp. D1; Fig. 1, the result quoted from Brewer & Kueck; cf. also certain measurements discussed in the paper of Cook) indicates also the comparatively common occurrence of very low ratios $^{39}K/^{41}K$, a fact which is not easily reconciled with a small fractionation in the emission from the 2 % coatings.

There remains, however the necessity of explaining the disagreement as to the initial ratio, $q(0)$. According to the accepted explanation, this should be equal for thick and thin coatings (and for the atomic-beam source with fluid contents of the crucible). It is necessary to postulate mass discrimination larger than the theoretical (5 %, as compared to 2.5 %). Possibly, there are two molecular processes cascaded: the diffusion within the salt, and the evaporation from the surface. In thick coatings, the first-mentioned may acquire importance, but large variations are possible as a result of differences in structure of the coatings. In order to give a real cascading effect, the major part of the diffusive transport must be directed into some third, not mass-selective, process, maybe a transport by grain boundaries, resulting in crystal growth. In the atomic-beam experiments, steady-state conditions were probably not obtained, and cascaded fractionation has probably occurred.

(3) Considering the various implications of these two interpretations of the data obtained, it seems not possible to make a specific choice without recourse to other information available. In view of the low values obtained in the recent determinations by electron-impact ionization, the thin coatings rather than the thick ones would be preferred in determining the integral ratio; assuming that in fact no appreciable loss of sample from the filament occurred during the exhaustion runs, the resulting value is, $Q = 13.50$, yet to be corrected for instrument and method errors.

V.5. Evaluation of the ratio, ^{39}K/^{41}K

The directly measured initial ratio has to be corrected according to the survey of Sect. III.6. Additionally, there is a correction due to the varying efficiency of ionization during the consumption of the sample. In Appendix 2 the theory of this correction is worked out, on the assumption that the only cause of this variation is the gradual increase of temperature necessary to compensate for the decrease in quantity of the sample. According to eq. (I.1) there are also other parameters involved, viz. the electron work function and the heat of evaporation, which are liable to change with the state of the coating. Thus, the course of the ratio i_+/i_0 cannot be stated in detail. However in the case of the thin coatings, the emissivity has really varied through the major part of the run, approximately as postulated in the theory, viz. proportional to the remaining quantity, as realized by inspection of Fig. 12. The high values of emissivity at the beginning of the run are thought to be immaterial; the somewhat high values towards the end are probably the result of the return of substance migrated into the filament. Accordingly, it is probable that the theory is applicable for a rough estimation of this effect.

According to eq. (A2.4), the experimentally observed discrimination, α^*, has to be multiplied by $h/(g+h)$ in order to give the true discrimination, α. Here h gives the power of temperature, by which the rate of evaporation of neutral atoms varies, and g the power correspondingly related to the degree of ionization, $\varkappa$. Eq. (A2.6) gives: $g = -\ln \varkappa$, when $\varkappa \ll 1$. Furthermore, according to (V.4), the variation of the emission with filament current can be put proportional to I_f^{70}, for $I_f = 5$ A. Measurements with an optical pyrometer showed the temperature to vary as $I_f^{2.7}$. Thus, the temperature dependence of the ion evaporation is approximately represented by the power, T^{30}, the exponent being equal to $g+h$. The considerations of Sect. V.4B indicate, that the degree of ionization was about 2 %, whence $g = 4$, and the correction to α measured, $-0.1\ \alpha$.

The percentage corrections and limits of error (p.e.) are listed below:

$q(0)$ measured	$13.87 \pm 3_5$
Q measured	13.50 ± 3
α measured, %	2.70 ± 40
instrument corrections (Sect. III.6)	$+0.25 \pm 45$ %
electrical calibration error	0.00 ± 10 %
$q(0)$ corrected	13.90 ± 7
incomplete ionization correction	$+0.25 \pm 30$ %
sum of corrections to Q measured	$+0.50 \pm 55$ %
Q corrected	13.57 ± 9

VI. Measurement of the ratio, $^{39}K/^{40}K$

VI.1. Introductory remarks

The result of the measurements on ^{40}K were reported in R I, together with an account of the principles of the method employed for eliminating the mass discrimination inherent in the source and the instrument. In the following sections, the underlying data will be presented, and a new, more exact, evaluation of the ratio, $^{39}K/^{40}K$, will be carried out.

The peaks were measured on automatic records of the mass spectrum, obtained by varying the ion energy (sample spectra are given in R I). Since the peak of ^{40}K appears superposed on the "tails" of the neighbouring peaks, it is necessary to reduce the scattering of the ion beams as far as possible, by operating at a good vacuum. From the slope of the fringes, the gas pressure could be estimated (cf. Ehrenberg). The smallest pressure read on the vacumeter was 0.7 μTorr; when operating with the manometer shut off, the pressure would ultimately decrease to 0.3 μTorr. This background is efficiently reduced by diminishing the collector slit width; however, the peaks becoming narrower, the exact height measurement is made more difficult. Also, risks of discrimination by space-charge defocusing increase.

Measurements were, accordingly, made both with the ordinary width (0.7 mm) at the selector slit, and with a narrow one (0.3 mm, about the same as the entrance slit). With the wide slit, the peak tails are curved within the base of the peak ^{40}K, and the course of the background must be guessed and drawn into the record by hand; this might introduce a personal error of measurement. The peak ^{40}K had to be scanned with the maximum sensitivity of the amplifier; thus the reading of the maximum height is easily affected, in the case of a narrow selector slit, by the "noise" appearing in the record. The mass sweep must thus be made rather slow; in addition, it had to be interrupted some tens of seconds when changing the resistor before scanning the 40 peak, because of a large transient occurring in the amplifier. Different speeds were tried, and two different recorders employed (see Sect. II.8).

In order to make possible an analysis of the systematic errors made in different experimental arrangements, each series of measurements was treated statistically for the purpose of establishing the random errors. For the average value, the median was taken—which makes the result largely independent of extreme individual deviations, which can occur as a result of sudden changes of emission current, etc. It was then realized, that the current method of obtaining the error of the mean by dividing the individual deviations by the square root of the number of individual observations, would give too narrow limits, because the deviations of the individual observations could not be considered as uncorrelated. In fact, the deviations reflect changes in the state of the apparatus, in particular the emitting coating of the filament; the rate of change is slower than the rate of repetition of observations, the chance of two consecutive deviations having the same sign thus being greater than $\frac{1}{2}$. A simple way of dealing with this phenomenon is to introduce a quantity which will be called *the effective number of observations*; it will be put equal to twice the number of changes of sign of deviation in the time-series of observations. This method is theoretically sound, if the deviations are mainly due to either the variations in state of the object investigated, or the measuring errors. In the intermediate range of competing sources of variations, it gives too small error limits; however the data are insufficient for a more detailed statistical treatment.

VI.2. Procedure of measurement, and results

A. Experiments D1 and D2

In exp. D1 (date, 9/2), the filament coating (powdered K_3PO_4) was rather depleted by previous experiments, a freshly-prepared coating being, however, employed in the other experiment (date, 1/3). A wide selector slit was used. The spectrum was scanned alternatingly in both directions, employing the "EA" recorder. The isotopes 39 and 41 were recorded with the resistor R_1 in the ranges 10 V and 1 V, resp., the isotope 40 with R_3 in 0.1 V. The records were placed on top of a light-box, which was covered by a piece of record chart, carrying a curved line, embodying the curved ordinate axis of the record; thus top and background of the 40 peak could be read out properly, irrespective of the strong slopes caused by the underlying peak tails. The ordinate line was obtained by letting the galvanometer pen swing across the whole scale; the printed coordinate lines are not to be relied upon. From the corrected meter deflexions, the meter current ratios I_{39}/I_{41}, and I_{39}/I_{40}, were obtained for each spectrum. Consecutive spectra were grouped in pairs (1 and 2, 2 and 3, etc.) and the means of the ratios taken. The ratios, I_{39}/I_{40}, obtained were then multiplied by the relevant ratio of voltage ranges, and the corrections, α_{13},[1] to the standard value, $Q_{13} = 13.57$, obtained for every pair of spectra; then the ratio I_{39}/I_{40} was corrected by the corresponding $\alpha_{12} = \frac{1}{2}\alpha_{13}$, giving individual ratios which were free from the instrument discrimination, as well as from effects of a constant drift of ion source emission intensity. These ratios were treated statistically, the appropriate scale factors applied, and the results entered in Table 5.

B. Experiment D3

The selector slit was now exchanged for a narrow one. The measurements are grouped into three series (date, 13/3):

Series I.—The recorder chart was fed continuously, the record thus providing a correct time-scale for eliminating linear drifts of peak intensity by means of interpolation. The mass sweep, as usual, was interrupted for from 0 to 6 seconds before recording the 40 peak. The continuous sweep was 1 mass unit in 12 seconds.

Series II.—The chart feed was, as usual, kept in step with the mass sweep; the intervals of interruption were in part, short (just the time necessary for switching the resistors and voltage ranges), in part 10 to 20 seconds longer. The dependence of the ratio, q_{12}, on the length of this interval did not stand out very clearly; maybe the transients resulted in a ratio too high by $0.25 \pm 25\,\%$. No consideration was given to this, and a common mean was taken for the whole of this series.

Series III.—The record was obtained by "HB", the procedure being the same as in series II. The sweep speed had to be reduced to 1 MU in 30 seconds.

C. Discussion of the result, $^{39}K/^{40}K$ (Table 5)

In order to give a picture of the magnitude of the corrections involved in evaluating the measurements, the top of the table gives a calculation of the discriminations, α_{13}, occurring in the various series of measurement; they are obtained from the medians of the ratio i_{39}/i_{41} in each series. These α's, however, have no significance in the evaluation of the results, Q_{12}, since these were primarily obtained individually

---

[1] For a definition of α, see Sect. V. 1; the subscripts 1, 2, 3, refer to the isotopes 39, 40, 41.

Table 5. Determinations of the ratio $^{39}K/^{40}K$.

Exp. no.	D1		D2	D3		
Series no.	I	II		I	II	III
R_3/R_1 (Sect. II.8)	71.17		71.79	71.74		
$q_{13} = i_{39}/i_{41}$, median	13.41	13.41	14.26	14.37	14.34	14.33
α_{13}, %	+ 1.2	+ 1.2	− 4.8	− 5.6	− 5.4	− 5.3
Q_{12}, median	7951	7931	7931	7892	7906	7924
Dev. of indiv. obs., median	±30	±36	±44	±50	±36	±60
Number of obs.	22	10	14	19	19	9
Effective number of obs.	14	10	14	18	9	4
p.e. of Q_{12}	±8	±12	±12	±12	±12	±30
Means of Q_{12}	7950 ± 7		7940	7910 ± 9		
	7945 ± 7					
	7935 ± 11					

for each pair of spectra recorded, as explained in the account, in Sect. A. The medians of these are thus entered directly, with appertaining statistical data.

In the final taking of means, the series are grouped according to slit widths. The disagreement between these means is such, that one has to induce the existence of a factor which was not considered in their evaluation and the establishing of error limits. *One* may be the instability of the ratio R_3/R_1, which well might introduce an indeterminacy of the required magnitude, 0.35 %. On the other hand, with narrow peaks the maximum height of the 40 peak might have been taken too high, as a result of the "noise" in the record; accordingly, Q_{12} of D3 would come out lower, which is in the sense actually observed. Furthermore, the 39 peak might have become about 0.1 % too low as a result of space-charge defocusing; this would have an effect in the same sense. Such phenomena are not active in the measurements obtained with a wide collector slit, and it appears plausible that these are to be given a greater weight because of their smaller random deviations, in spite of the difficulty of interpolating the background under the 40 peak. Accordingly, as a final mean, is chosen $Q_{12} = 7935$. The total limits of error have to include the random error (± 11), the error in calibrating the ratio of the voltage ranges, 10 V to 0.1 V, (± 0.1 %), and half of the errors in Q_{13} (± 0.55 %) and in the voltage range calibration, 10 V to 1 V, (± 0.1 %), which are introduced by the method of eliminating the mass discrimination. The result is thus: $^{39}K/^{40}K = 7935 \pm 30$ (p.e.). Allowing for future changes in the value of the calibrating ratio, $^{39}K/^{41}K = Q_{13}$, the result of the measurements reported in this chapter may be summarized in the following way:

$$Q_{13} = (1 + \alpha_{13})\, i_{39}/i_{41};$$

$$Q_{12} = (1 + \tfrac{1}{2}\alpha_{13})\, i_{34}/i_{40}.$$

Hence, inserting the numerical result in the case of $Q_{13} = 13.57$, one obtains: $Q_{12} = {}^{39}K/^{40}K = 7935 \pm 15 + 280\,(Q_{13} - 13.57)$.

Incidentally, it is interesting to note that the condition of the emitting coating plays a rather unimportant role in this determination, thanks to the method of calibrating the instrument. The source of exp. D1 was so exhausted, that the correction, k, became very small; the corrected result, nevertheless, agrees sufficiently with the other determinations to justify the procedure of putting $\alpha_{12} = \frac{1}{2}\alpha_{13}$. The isotope discrimination of the source is really a mass effect.

Appendix 1. Space-charge corrections to peak ratio measurement

In an ion beam of rectangular cross-section, $h \times 2y$ $(h \gg 2y)$, let the total current be I, and the ion velocity v. The electric field intensity causing the widening in the y direction (median plane), is at the beam boundary: $2\pi I/hv$ (Gaussian unit system). Further, there is a magnetic flux B parallel to the coordinate of h. In polar coordinates, $r = a \pm y$, $(y > 0)$, $\varphi = s/a$, the equations of movement at the inner and outer boundaries of the beam, for ions of mass m and charge e, become:

$$\pm m\ddot{y} = mv^2/(a \pm y) - evB/c \pm 2\pi eI/hv. \tag{A1.1}$$

Take a = radius of curvature in the undisturbed field, B, where $a = mvc/eB$; assume $a \gg y$, and develop the first dextral term in powers of y/a, breaking off after the first member. Denote further:

$$\gamma = \frac{2\pi a e I}{h m v^3}. \tag{A1.2}$$

The result is: $\ddot{y} + (v/a)^2 y = v^2\gamma/a$, whence:

$$y(s) = a\alpha \sin\frac{s}{a} + a\gamma\left(1 - \cos\frac{s}{a}\right),$$

the equation of path which satisfies the boundary conditions imposed at the first slit: $s = 0$, $y = 0$, $dy/ds = \alpha$; thus, α denotes the angular half-aperture of the beam at the first slit.

At the focus, y is independent of α, which condition gives:

$$\sin\frac{s}{a} = -\frac{\gamma}{\alpha}\left(1 - \cos\frac{s}{a}\right).$$

Since $\gamma \ll 1$, $s/a \approx \pi$. Denote $s/a = \pi + \theta$, $|\theta| \ll 1$; then $\theta = 2\gamma/\alpha$. Accordingly, space-charge displaces the focus a length, which to the first order of approximation is given by $a\theta = 2a\gamma/\alpha$ (Robinson).

In front of the selector slit, every element of the image of the first slit is widened by the amount $\delta = 2\alpha a\theta = 4a\gamma$. If the slits have the same width, a/M (M denoting the geometric mass resolution), then the relative loss of intensity is $\lambda_1 = \delta M/4a = M\gamma$. Passing to e.m.u., the formula expressing the relative loss of collector current through displacement of focus due to space charge in the beam, is:

$$\lambda_1 = M\gamma;\ \gamma = \frac{\pi m c^2 I}{BeUh}. \tag{A1.3}$$

Actually the error of measurement of isotopic abundance is less, due to the following causes:

(1) The beam height, h, is not in all places $\gg$ the width, $2y$, as assumed in deriving (A1.1). Only part of the charge is effective in the y coordinate. Becker & Walcher give a diagram on the efficiency of space-charge in widening the beam, as functio of the cross-section ratio, $2y/h$. For instance, in the case of $h/2y = 3$, one obtains a correcting factor to γ, $C_1 = 0.8$.

(2) Not the intensity of ion current, but the ratio of intensities is measured, and the error effective is not λ_1, but the difference, $\Delta\lambda_1$, of two relative intensity losses (supposed small). The space-charge is essentially caused by the main isotope; but the isotopic beams being mixed up nearly all the way between the slits, the weaker isotope also experiences loss of focusing. Detailed ion optical considerations (Becker & Walcher) yield the result that a little less than half of the main isotope effect is transferred to the weak isotopes, if the isotopic beams are wholly separated just before the selector slit. As a rough estimate, this may be considered as the case present in a 180° spectrometer; thus the expression for the space-charge effect on the ratio measurement becomes:

$$\Delta\lambda_1 = \tfrac{1}{2} C_1 M \gamma \text{ (equal slit widths).} \tag{A1.4}$$

There is one more space-charge effect, the widening of the beam in the h (or magnetic flux) direction, giving the relative intensity loss, λ_2, due to lack of focusing in this direction. Starting with the expression: $2\pi I/2yv$, giving the electric field intensity at the h boundaries of the beam, one obtains, as an analogue of (A1.1):

$$2\Delta = \tfrac{1}{2}\pi^2 a h \gamma / y, \tag{A1.5}$$

giving the increase of beam height at the selector slit. The corresponding relative loss of intensity will then be less than $2\Delta/h_{\text{stop}}$, the numerator being the height of the relevant stop just in front of the selector slit (*11* of Fig. 2). Disregarding the difference of h_{stop} from h in (A1.5)—which is understood to denote an average height between the slits—one obtains:

$$\lambda_2 \leq \tfrac{1}{2}\pi^2 a \gamma / y.$$

Introducing, as before, a correction factor, C_2, for the limited ratio $2y/h$, and the factor $\tfrac{1}{2}$, on account of transfer of space-charge widening to the weak isotope beam, the error in ratio measurement becomes:

$$\Delta\lambda_2 \leq \tfrac{1}{4}\pi^2 C_2 a \gamma / y. \tag{A1.6}$$

Appendix 2. Correction to integral ratio measured, due to incomplete ionization

The fundamental equation of abundance ratio as function of evaporated fraction, (V.1), strictly applies to the total emission of ions and atoms. In the experiments, the charged part, only, of the emission is measured, and this is not a constant fraction throughout each experiment, as the temperature is controlled to keep the emission at an approximately fixed value. The discrimination, α, thus obtained, will then be in error; it may be corrected by means of the following considerations.

It will be assumed, that the degree of ionization be small: $\varkappa \ll 1$, the differential of ion charge emitted being denoted by $d\xi = \varkappa\, dx$. Approximating the temperature functions of ionization and rate of evaporation by powers of T, one obtains:

$$\varkappa = \mathrm{K}\, T^{g}, \tag{A2.1}$$

$$\frac{dx}{dt} \approx (1-\varkappa)\frac{dx}{dt} = \mathrm{X}(1-x)\,T^{h}, \tag{A2.2}$$

X being an emissivity constant related to E of eq. (V.4). Hence, the emission current,

$$\frac{d\xi}{dt} = \mathrm{K}\,\mathrm{X}(1-x)\,T^{g+h}, \tag{A2.3}$$

being fixed at the value J, gives T in terms of x. Inserting in (A2.1), one obtains the equation

$$\frac{d\xi}{dx} = \mathrm{K}\cdot\left[\frac{J}{\mathrm{K}\,\mathrm{X}(1-x)}\right]^{\frac{g}{g+h}},$$

which, by integration between the limits $\xi(0)=0$, $\xi(1)=\xi_1$, yields ξ_1, the fraction of sample which is emitted as ions. With the notation $x^* = \xi/\xi_1$, there results

$$1 - x = (1 - x^*)^{1+g/h}.$$

x^* is the experimental counterpart of x, as ions only are recorded. Accordingly, the fundamental equation, (V.1), by which the discrimination α is obtained, can be written

$$q = q(0)(1-x^*)^{\alpha^*},\quad \alpha^* = \alpha(1+g/h). \tag{A2.4}$$

The ratio g/h is, in general, not known, but it can be estimated as follows: from (I.1), where $i_+/i_0 = \varkappa/(1-\varkappa)$, one obtains

$$\varkappa = (1+e^{b/T})^{-1}, \tag{A2.5}$$

whence

$$g = \frac{d\ln\varkappa}{d\ln T} = \frac{b}{T}(1+e^{-b/T})^{-1}.$$

Thus $\varkappa$ and g are related in the following way:

$$g = (1-\varkappa)\ln\left(\frac{1}{\varkappa}-1\right) \approx \ln\frac{1}{\varkappa},\quad \varkappa \ll 1. \tag{A2.6}$$

Summary

1. The method of mass spectrometer calibration by synthetic samples, as applied by Nier (1950) to the investigation of potassium, cannot—from the data published—be granted to have eliminated the instrumental errors. (Sect. I.3.)

2. The hot anode ion source of Brewer (1936a), which employs the ion emission from platinum impregnated with alkali, probably exhibits mass discrimination, which cannot be eliminated through making measurements by integrating ion currents. The coated filament should be preferred for such experiments. (Sect. I.4.)

3. The construction of an all-metal mass spectrometer of the 180° focusing type is described. Special features are a mechanical device for directing the ion beam, and a vacuum lock for rapid exhange of filaments. (Sect. II.2.)

4. An account is given of the auxiliary equipment employed. An automatic switching device with a null detecting galvanometer in the output circuit of the isotope-current amplifier converts the single-beam spectrometer into a ratio-measuring instrument. (Sects. II.3–8.)

5. The instrumental errors are investigated experimentally and theoretically. The largest uncertainty remaining is due to deformation of the filament by magnetic forces, which would be rendered harmless by introducing double-directional focusing. (Chapter III.)

6. Measurements on powdered leucite give, in agreement with Brewer's (1936b), the ratio of ^{39}K to ^{41}K, 14.20. Diluted solutions of pure potassium salts, however, give lower values. With coatings containing less than 5 μg potassium to the mm^2, the ratio is 13.88 ± 7 (p.e.).

7. With a specimen of a Pacific kelp (Macrocystis pyrifera), using the extract by water of the ashes directly, the average ratio obtained was 13.67 ± 8 (p.e., considering only errors relative to the standard value, 13.88). A sample of sea water, after chemical separation of the potassium, however, gave 14.06 ± 4. This difference is in qualitative agreement with the results obtained by Brewer (1936b). (Sect. IV.3.)

8. After purifying chemically the potassium salt in the extract of the kelp ashes, the ratio obtained rose to 13.94 ± 3. This figure is taken to be more significant of the isotopic constitution of the potassium in kelp than the first-mentioned, the inference being that admixture of chemicals to the potassium salt affects the isotope fractionation in the emission of ions. The conclusion is supported by other experiments with coatings of varying purity. Such effects are understood by considering the diverse types of diffusion possible in the source employed. (Sect. IV.3.)

9. Ion currents were integrated in order to determine isotope-ratio free from source fractionation. With coatings containing about 0.5 μg of potassium on the mm^2, the enrichment of the heavier isotope is in good agreement with that of free molecular effusion. After correcting for a probable variation in the degree of ionization of the potassium evaporated, the ratio ^{39}K/^{41}K is obtained as 13.57 ± 9. (Sect. V.5.)

10. With thicker coatings, the enrichment of ^{41}K during consumption of the ion source proceeds in an irregular course. Reasons are presented for the surmise that, with the point-by-point ratio-measuring technique employed, the measurements on such coatings will not give a true average of the isotopic ion currents. The measurements would thus be consistent with a true abundance ratio of 13.88, or a still lower one. (Sect. V.4.)

11. A full explanation of the disagreement of the results obtained on thin and thick coatings, and a definite decision regarding the true value of the ratio, $^{39}K/^{41}K$, cannot be given on the basis of the data obtained; for this, it is necessary to calibrate the spectrometer by synthetic isotope mixtures of potassium. (Sect. V.4.)

12. The data of the determination of the isotopic abundance of ^{40}K, published previously (Reuterswärd 1951 b), are presented, and a new evaluation given, the result being:

$$^{39}K/^{40}K = 7935 \pm 15 + 280\ (^{39}K/^{41}K - 13.57). \qquad \text{(Sect. VI.2.)}$$

13. The space-charge corrections to peak-ratio in a 180° spectrometer are derived from theory.

14. The theory of the correction mentioned in par. *9* is given.

REFERENCES

ANGERER, E. v., Technische Kunstgriffe bei physikalischen Untersuchungen. (F. Ungar, New York.)
BARNARD, G. P. (1953), Modern Mass Spectrometry. (The Institute of Physics, London.)
BECKER, E. W. and WALCHER, W. (1952), Z. Physik *131*, 395–407.
BERRY, C. E. (1950), Phys. Rev. *78*, 597–605.
BONDY, H. and VANICEK, V. (1936), Z. Physik *101*, 186–192.
BREWER, A. K. and KUECK, P. D. (1934), Phys. Rev. *46*, 894–897.
BREWER, A. K. (1935), Phys. Rev. *48*, 640.
—— (1936 a), J. Chem. Phys. *4*, 350–353.
—— (1936 b), J. Am. Chem. Soc. *58*, 365–370.
—— (1936 c), J. Am. Chem. Soc. *58*, 370–372.
—— (1937), J. Am. Chem. Soc. *59*, 869–872.
BRÜCHE, E. and SCHERZER, O. (1934), Geometrische Elektronenoptik. (Springer, Berlin.)
CHEMLA, M. and SUE, P. (1953), C. r. (Paris) *236*, 2397–2399.
COLLINS, T. L. and ROURKE, F. M. (1953), KAPL-999, 1–22.
COOK, K. L. (1943), Phys. Rev. *64*, 278–293.
COPLEY, M. J. and PHIPPS, T. E. (1935), Phys. *48*, 960–968.
DAVISSON, C. J. and CALBICKS, C. J. (1932), Phys. Rev. *42*, 580.
EHRENBERG, H. F. (1953), Z. Physik *134*, 317–333.
EISENSTEIN, A. S. (1948), Adv. Electronics *1*, 1–130.
GRÁF, T. (1948), Phys. Rev. *74*, 831.
HERZOG, R. (1934), Z. Physik *89*, 447–473.
HUNT, F. V. and HICKMAN, R. W. (1939), Rev. Scient. Instr. *10*, 6–21.
INGHRAM, M. G. (1946), Phys. Rev. *70*, 653–660.
INGHRAM, M. G. and CHUPKA, W. A. (1953), Rev. Scient. Instr. *24*, 518–520.
JONES, T. J. (1936): Thermionic Emission. (Methuen, London.)
KOLTHOFF, I. M. and SANDELL, E. B. (1943): Textbook of Quantitative Inorganic Analysis. (McMillan, New York.)
KLEMM, A. (1953), Z. Naturforsch. *8a*, 397–400.
LU, H. (1938), Phys. Rev. *53*, 845–846.
LUNDÉN, A., REUTERSWÄRD, C., and LODDING, A. (1955), Z. Naturforsch. *10a*, 924–926.
MANLEY, J. H. (1936), Phys. Rev. *49*, 921–924.
MILLER, S. E. (1941), Electronics, Nov., 27–31, 105–109.
NIER, A. O. (1935), Phys. Rev. *48*, 283–284.
—— (1947), Rev. Scient. Instr. *18*, 398–411.
—— (1950), Phys. Rev. *77*, 789–793.
PAUL, W. and PAHL, W. (1944), Naturwiss. *32*, 228–229.
PLOCH, W. (1951), Z. Physik *130*, 174–195.
PLOCH, W. and WALCHER, W. (1950), Z. Physik *127*, 274–288.
—— (1952), Rev. Scient. Instr. *22*, 1028.
REIMANN, A. L. (1934): Thermionic Emission. (Wiley, New York.)

REUTERSWÄRD, C. (1947), Ark. Mat. Astr. Fysik *34A*, no. 29, 13–14.
—— (1951a), Ark. Fysik *3*, 53–62.
—— R I (1951b), Ark. Fysik *4*, 203–205.
—— (1955), Swedish National Conf. Physics, Stockholm.
—— R II (1956), Ark. Fysik *10*, 501–524.
ROBINSON, C. F. (1949), Rev. Scient. Instr. *20*, 745.
SEITZ F. (1940): The Modern Theory of Solids. (McGraw-Hill, New York.)
—— (ed.) (1952): Imperfections in Nearly Perfect Crystals. (Wiley, New York.)
SHERWIN, C. W. (1940), Phys. Rev. *57*, 814–821.
SMYTHE, W. R. and HEMMENDINGER, A. (1937), Phys. Rev. *51*, 178–182.
WAGENER, S. (1943): Die Oxydkathode, *T*. 1. (Barth, Leipzig.)
WALLENQUIST, Å. (1954), K. Svenska Vet.-Akad. Handl. (IV) *5*, No. 5.
WHITE, J. R. and CAMERON, A. E. (1948), Phys. Rev. *74*, 991–1000.

Tryckt den 26 april 1956

Uppsala 1956. Almqvist & Wiksells Boktryckeri AB